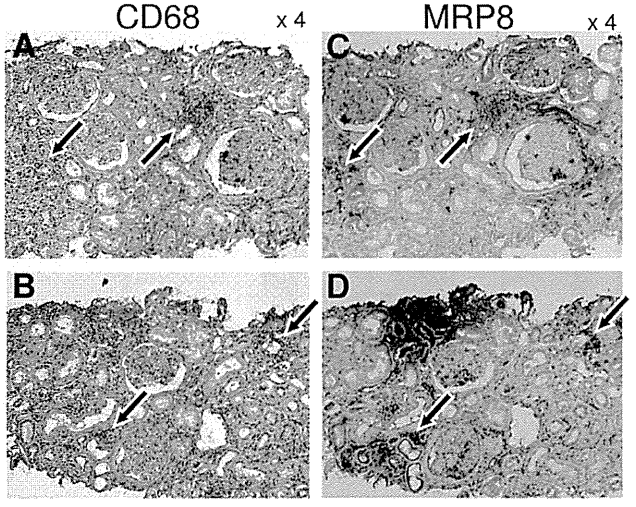

Figure 2. Localization of CD68 and MRP8 protein expression in serial sections of diabetic nephropathy cases. Expression of CD68 (A, B) and MRP8 expression (C, D) in paired renal specimens (A and C, or B and D). Arrows indicate colocalization of CD68 and MRP8 signals.
doi:10.1371/journal.pone.0088942.g002

levels tended to be higher than MGA or MCNS subjects. In baseline cross-sectional investigation including all subjects, by univariate linear regression analysis, glomerular MRP8-positive cell count and tubulointerstitial MRP8-positive area were both, respectively, correlated not only with various known risk factors for diabetic nephropathy (such as systolic blood pressure, proteinuria and serum creatinine) but also with extent of glomerulosclerosis and tubulointerstitial fibrosis. By multivariate analysis, tubulointerstitial MRP8-positive area was significantly correlated with proteinuria and tubulointerstitial fibrosis. Glomerular MRP8-positive cell count was significantly correlated with tubulointerstitial fibrosis in the primary analysis, and with proteinuria in a sub-analysis excluding MCNS group. Immunohistochemistry indicated that MRP8 was expressed, at least partly, by CD68(+)-expressing macrophages and atrophic tubules. These findings raise a possibility that kidney MRP8 signals in glomeruli or tubulointerstitium may serve as novel markers of diabetic nephropathy.

In prognostic study, multivariate analysis revealed that urinary protein levels at a year after renal biopsy were independently associated with glomerular MRP8-positive cell count, urinary protein and systolic blood pressure at baseline. Of note, glomerular MRP8 expression showed the strongest correlation with urinary protein a year later ($\beta = 0.87$), even stronger than baseline urinary protein ($\beta = 0.78$), by univariate analysis. It is partly because glomerular MRP8 expression is not largely elevated in 'benign' forms of proteinuria such as ones observed in MCNS patients, whose levels of proteinuria are extremely high at diagnosis by renal biopsy but are usually resolved within a year after initiation of immunosuppressive therapy. These findings suggest that glomerular MRP8 expression may possess a unique predictive nature as a disease marker, which cannot be substituted by baseline proteinuria or routine pathological analysis evaluating

Table 3. Relationship between baseline clinical parameters and MRP8 signals.

	Glomerular MRP8-positive cell count				Tubulointerstitial MRP8-positive area			
	Univariate		Multivariate*		Univariate		Multivariate#	
	β	P	β	P	β	P	β	P
Sex (male)	0.21	0.09			0.16	0.20		
Age (y)	0.37	0.002	0.02	0.87	0.39	0.001	0.03	0.74
Diabetes duration (y)	0.28	0.14			0.33	0.08		
BMI (kg/m^2)	0.14	0.27			0.09	0.48		
HbA1c (NGSP, %)	0.11	0.52			0.04	0.82		
Systolic BP (mmHg)	0.62	<0.001	0.18	0.29	0.64	<0.001	−0.12	0.37
Diastolic BP (mmHg)	0.43	<0.001			0.42	<0.001		
Urinary protein (g/gCr)	0.37	0.003	0.18	0.07	0.43	<0.001	0.20	0.01
Creatinine (mg/dl)	0.60	<0.001	0.01	0.10	0.75	<0.001	0.20	0.08
eGFR (ml/min/1.73 m^2)	−0.49	<0.001			−0.70	<0.001		
BUN (mg/dl)	0.56	<0.001			0.71	<0.001		
Total protein (g/dl)	−0.16	0.21			−0.13	0.30		
Albumin (g/dl)	−0.22	0.09			−0.21	0.09		
T-chol (mg/dl)	−0.06	0.66			−0.04	0.76		
Triglyceride (mg/dl)	0.02	0.84			0.11	0.38		
HDL-chol (mg/dl)	−0.24	0.06			−0.28	0.03	−0.03	0.73
LDL-chol (mg/dl)	0.00	0.98			0.00	0.99		
CRP (mg/dl)	0.03	0.79			0.12	0.34		
Global GS (%)	0.52	<0.001	−0.17	0.40	0.61	<0.001	−0.27	0.07
TI fibrosis (%)	0.68	<0.001	0.62	0.02	0.80	<0.001	0.85	<0.001

Coefficient of determination (R^2) calculated with explanatory parameters enrolled in multiple regression analysis was 0.52* and 0.74#, respectively. y, years; BP, blood pressure; gCr, g creatinine; T-chol, total cholesterol; HDL-chol, HDL cholesterol; LDL-chol, LDL cholesterol; GS, glomerulosclerosis; TI, tubulointerstitial.
doi:10.1371/journal.pone.0088942.t003

Table 4. Sub-analysis of relationship between baseline clinical parameters and MRP8 signals, after exclusion of MCNS group.

	Glomerular MRP8(+) cell count				Tubulointerstitial MRP8(+) area			
	Univariate		Multivariate*		Univariate		Multivariate#	
	β	P	β	P	β	P	β	P
Systolic BP (mmHg)	0.64	<0.001	0.16	0.38	0.63	<0.001	−0.16	0.23
Urinary protein (g/gCr)	0.70	<0.001	0.36	0.03	0.75	<0.001	0.47	<0.001
Creatinine (mg/dl)	0.62	<0.001	0.05	0.80	0.75	<0.001	0.24	0.09
Total protein (g/dl)	−0.51	<0.001	0.03	0.84	−0.49	<0.001	0.12	0.25
Triglyceride (mg/dl)	0.31	0.003			0.37	0.01		
HDL-chol (mg/dl)	−0.16	0.27			−0.20	0.18		
LDL-chol (mg/dl)	0.60	<0.001	0.13	0.35	0.52	0.001	−0.10	0.35
Global GS (%)	0.49	<0.001	−0.20	0.29	0.59	<0.001	−0.17	0.23
TI fibrosis (%)	0.68	<0.001	0.38	0.18	0.80	<0.001	0.70	0.002

R^2 was 0.60* and 0.77#, respectively. BP, blood pressure; gCr, g creatinine; HDL-chol, HDL cholesterol; LDL-chol, LDL cholesterol; GS, glomerulosclerosis; TI, tubulointerstitial.

doi:10.1371/journal.pone.0088942.t004

Table 5. Multiple regression analysis for identification of factors predicting urinary protein levels 1 year after renal biopsy.

	Urinary protein 1-year after renal biopsy					
	Univariate		Multivariate			
			Model 1*		Model 2#	
	β	P	β	P	β	P
Sex (male)	−0.14	0.50				
Age (y)	−0.01	0.95				
Diabetes duration (y)	0.24	0.22				
BMI (kg/m$^{2)}$	−0.33	0.10				
HbA1c (NGSP, %)	0.08	0.70				
Systolic BP (mmHg)	0.43	0.03	0.21	0.04	0.30	0.10
Diastolic BP (mmHg)	0.07	0.73				
Urinary protein (g/gCr)	0.78	<0.001	0.37	0.002	0.55	0.002
Creatinine (mg/dl)	0.44	0.02				
eGFR (ml/min/1.73 m^2)	−0.56	0.003	−0.31	0.76	0.18	0.45
BUN (mg/dl)	0.46	0.02				
Total protein (g/dl)	−0.54	0.004				
Albumin (g/dl)	−0.69	<0.001				
T-chol (mg/dl)	0.66	<0.001				
Triglyceride (mg/dl)	0.18	0.38				
HDL-chol (mg/dl)	−0.02	0.91				
LDL-chol (mg/dl)	0.62	<0.001				
CRP (mg/dl)	−0.11	0.57				
Global glomerulosclerosis (%)	−0.05	0.79	−0.17	0.11	−0.31	0.06
Tubulointerstitial fibrosis (%)	0.43	0.02	−0.02	0.91	0.10	0.67
Glomerular MRP8(+) cell count	0.87	<0.001	0.59	<0.001		
Tubulointerstitial MRP8(+) area (%)	0.67	0.001			0.34	0.09

R^2 was 0.91* and 0.75#, respectively. y, years; BP, blood pressure; gCr, g creatinine; T-chol, total cholesterol; HDL-chol, HDL cholesterol; LDL-chol, LDL cholesterol.

doi:10.1371/journal.pone.0088942.t005

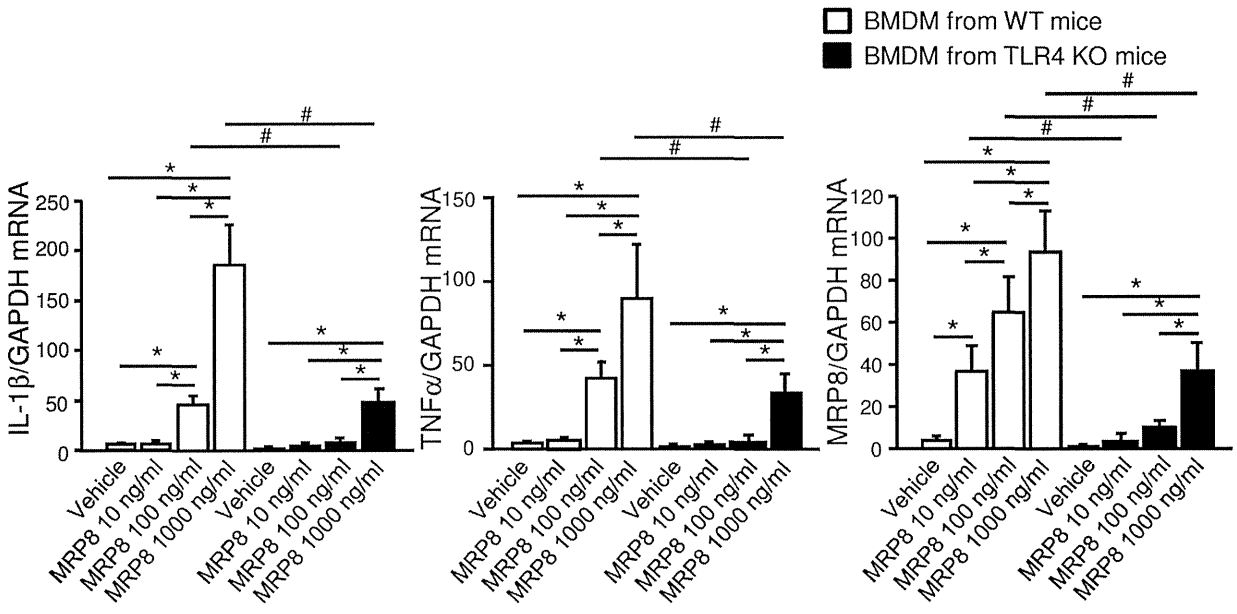

Figure 3. Effects of MRP8 upon bone marrow-derived macrophages. Bone marrow-derived macrophages (BMDM) were stimulated with recombinant mouse MRP8 for 4 hours. Error bars indicate 95% CI and statistical analyses were performed with log-transformed values. Two-way ANOVA revealed significant effects of genotypes, MRP8 concentrations and their interactions for expression of all 3 genes ($P<0.001$ for all comparisons). n = 4. WT, wild-type; KO, knockout; IL-1β, interleukin 1 beta; TNFα, tumor necrosis factor alpha. *$P<0.01$ among different concentrations, #$P<0.01$ among genotypes.
doi:10.1371/journal.pone.0088942.g003

global glomerulosclerosis and tubulointerstitial fibrosis. Moreover, we speculate that glomerular MRP8 expression is not a simple marker or bystander but an active player in glomerular injury as discussed below.

In another attempt of longitudinal study, logistic regression analysis failed to find out any independent predictors for the occurrence of renal event within a year. We speculate that this is partly because tubulointerstitial MRP8 expression and tubulointerstitial fibrosis were two potent predictors for renal event in univariate analysis but their significances were canceled by each other in multivariate analysis. These two parameters showed strong correlation ($R = 0.68$, $P<0.001$) (Fig. S8), suggesting that these two parameters might be equivalent to predict renal event. Indeed, interstitial MRP8 expression showed quite similar pattern to interstitial fibrosis evaluated by Masson trichrome staining. Quantity of interstitial MRP8 largely depends on the positive signals in atrophic tubules rather than those in macrophages, whose feature differs from that of glomerular MRP8 in punctate distribution. Furthermore, small sample size, short observation period and few subjects who developed renal event might have reduced the detection power. Since MRP8 expression in tubular epithelial cells plays a causative role in the progression of tubulointerstitial inflammation in a mouse model of renal fibrosis [7], further analysis will be needed to clarify the role of tubulointerstitial MRP8 in DN.

In accordance with our previous study [6], MRP8 mRNA was upregulated predominantly in the glomerular fraction of human DN subjects as compared to control subjects with MGA. On the other hand, MRP8 protein expression was observed not only in the glomerulus but also in the tubulointerstitium. In this regard, it should be noted that there were two distinct patterns of MRP8 staining in the tubulointerstitium of DN. One was intense and focal staining in severely atrophic tubules. The other was mild staining distributed along the brush border of proximal tubules, which was also found in ORG and MCNS. The latter signals likely represent MRP8 protein derived from the blood and reabsorbed by proximal tubules, which should not be accompanied by increased MRP8 mRNA expression. Concerning proteins other than MRP8, we and others have recently reported similar phenomena of immunoreactive protein detection in the proximal tubules caused by reabsorption but not by renal synthesis [25,26]. On the other hand, since a little MRP8 staining remained in antibody absorption test, especially in glomerular exudative lesions and severely-scarred, fibrotic lesions around atrophic tubules, presence of non-specific signals cannot be completely negated (Fig. S3).

Glomerular MRP8 signals mainly showed punctuate pattern in DN subjects (Fig. 1, Fig. S4). Since both of CD68 and MRP8 were detected by mouse monoclonal antibodies, localization of these molecules were evaluated by serial sections, not by double-immunostaining. Staining patterns of MRP8 were compatible with those in other inflammatory renal disorders including IgA nephritis [27], membrano-proliferative glomerulonephritis [14], and ANCA-related glomerulonephritis [20], in which macrophages were suggested as a major source of MRP8, as we reported in a rodent model [6]. In addition, neutrophils could be considered as another source of MRP8 affecting vascular complications [28]. Currently, we are investigating the molecular mechanism why MRP8 is predominantly upregulated in myeloid-lineage cells infiltrating glomeruli. In vitro study revealed that MRP8 induced inflammatory cytokine expression and also potentiated expression of MRP8 itself in macrophages in a TLR4-dependent manner. Additionally, MRP8-positive cells were absent in nodular sclerosing lesion, suggesting that glomerular MRP8 might reflect ongoing glomerular damage [20]. Importantly, a largest-scale human study reported that MRP8 gene expression in blood mononuclear cells of type 1 diabetic patients is significantly elevated in subjects with diabetic complications including nephropathy [29].

Since inhibition of renin-angiotensin system (RAS) is an important determinant of renal outcomes, we examined the effects of RAS blockade on kidney MRP8 expression. We found no significant

difference in kidney MRP8 mRNA expression between DN patients treated with or without RAS blockade (Fig. S9), probably because cases treated with RAS blockade tended to have more severe hypertension and proteinuria than cases without RAS blockade.

In obese humans and mice, increased plasma MRP8/14 complex may reflect a degree of obesity and originate from adipocytes as well as leukocytes [8,9]. Our ORG cases had mild staining of MRP8 in proximal tubules, suggesting increased plasma levels of MRP8. In contrast, there was no significant correlation between tubulointerstitial MRP8 expression and body mass index (Fig. S6G). Therefore, local MRP8 expression in the kidney may serve better as a marker for renal injury rather than for obesity [8,9].

Our study has several limitations. Sample number of each group studied was small. Non-identical subjects were enrolled in the mRNA and immunohistochemical analyses. Since we only analyzed patients who underwent renal biopsy, the composition of patients investigated here may not reflect those in general type 2 diabetic patients or in general chronic kidney disease subjects. Although age was not retained as an independent factor associated with MRP8 signals in our data (Table 3), it is known that aging associates chronic inflammation [30]. The effects of age cannot be completely neglected. Although most MRP8 signals were lost in antibody absorption test, there were some positive signals remaining, which might be caused by a non-specific binding of the first antibody. As discussed above, investigation of renal MRP8 expression by renal biopsy helps us understand the pathophysiology and prognosis of chronic kidney diseases, especially associated with obesity and diabetes, but has a disadvantage for routine and repeated use in out-patient clinics.

In summary, the present study suggests that expression of MRP8 in the kidney reflects the current pathological status and also predicts renal outcomes in patients with obesity or type 2 diabetes. Further investigations studying urinary MRP8 levels among obese or diabetic patients in large scale may be warranted.

Supporting Information

Figure S1 Representative photos showing renal biopsy sections of a DN patient stained with (A) periodic acid-Schiff, (B) periodic-acid methenamine silver or (C) Masson trichrome. The ratio of the number of glomeruli with global sclerosis (arrows) among that of total glomeruli and the relative area of tubulointerstitial fibrosis were 33% and 65%, respectively, in this patient.
(TIFF)

Figure S2 Immunohistochemistry for MRP8 and CD68 proteins in DN patients. Photos in the right column show negative control experiments without 1st antibody.
(TIF)

Figure S3 Antibody absorption test for MRP8 staining. PBS: phosphate buffered saline, rhMRP8: recombinant human MRP8.
(TIF)

Figure S4 Representative photos of MRP8 expression in MGA, MCNS, ORG and DN groups.
(TIF)

Figure S5 Correlation between glomerular MRP8-positive cell count and clinical parameters. The log-transformed values of MRP8 signals were used. The correlations were analyzed using all of 4 groups (A–D, G) or 3 groups excluding MCNS group (E, F). Open circles: minor glomerular abnormality (MGA), closed circles: minimal change nephrotic syndrome (MCNS), open triangles: obesity-related glomerulopathy (ORG), closed triangles: diabetic nephropathy (DN).
(TIF)

Figure S6 Correlation between tubulointerstitial MRP8-positive area and clinical parameters. The log-transformed values of MRP8 signals were used. These correlations were analyzed using all of the 4 groups (A–D, G) or 3 groups excluding MCNS group (E, F).
(TIF)

Figure S7 Correlation between glomerular and tubulointerstitial MRP8 expression. The log-transformed values of MRP8 signals were used.
(TIF)

Figure S8 Correlation between tubulointerstitial MRP8-positive area and tubulointerstitial fibrosis. The log-transformed values of MRP8 signals were used.
(TIF)

Figure S9 Renal mRNA expression of MRP8 in DN patients with or without renin-angiotensin blockade. N.S.: not significant. n = 15 (Yes), 6 (No). Among 22 DN cases, information about medication was not available in one patient.
(TIF)

File S1 Supporting Tables. Table S1, Pathological diagnoses of all cases who underwent renal biopsy at Department of Medicine and Clinical Science, Kyoto University Hospital between 2000 and 2011. Table S2, Primer and probe sequences for TaqMan real-time RT-PCR. Table S3, Logistic regression analysis for the occurrence of renal event within a year.
(DOC)

Acknowledgments

We gratefully acknowledge S. Tanaka for statistical advice, Y. Ogawa, N. Igarashi and C. Kimura for technical assistance, and A. Yamamoto and S Ogino for secretary assistance.

Author Contributions

Conceived and designed the experiments: TK KM MK HY MI AN KN MM. Performed the experiments: TK HI AI KK TM YK MI AN. Analyzed the data: TK KM MK HY AS SY KU KN MM. Contributed reagents/materials/analysis tools: TK KM. Wrote the paper: TK KM MM.

References

1. Donath MY, Shoelson SE (2011) Type 2 diabetes as an inflammatory disease. Nat Rev Immunol 11: 98–107.
2. Odink K, Cerletti N, Bruggen J, Clerc RG, Tarcsay L, et al. (1987) Two calcium-binding proteins in infiltrate macrophages of rheumatoid arthritis. Nature 330: 80–82.
3. Vogl T, Tenbrock K, Ludwig S, Leukert N, Ehrhardt C, et al. (2007) Mrp8 and Mrp14 are endogenous activators of Toll-like receptor 4, promoting lethal, endotoxin-induced shock. Nat Med 13: 1042–1049.
4. Croce K, Gao H, Wang Y, Mooroka T, Sakuma M, et al. (2009) Myeloid-related protein-8/14 is critical for the biological response to vascular injury. Circulation 120: 427–436.
5. Loser K, Vogl T, Voskort M, Lueken A, Kupas V, et al. (2010) The Toll-like receptor 4 ligands Mrp8 and Mrp14 are crucial in the development of autoreactive CD8+ T cells. Nat Med 16: 713–717.
6. Kuwabara T, Mori K, Mukoyama M, Kasahara M, Yokoi H, et al. (2012) Exacerbation of diabetic nephropathy by hyperlipidaemia is mediated by Toll-like receptor 4 in mice. Diabetologia 55: 2256–2266.

7. Fujiu K, Manabe I, Nagai R (2011) Renal collecting duct epithelial cells regulate inflammation in tubulointerstitial damage in mice. J Clin Invest 121: 3425–3441.
8. Sekimoto R, Kishida K, Nakatsuji H, Nakagawa T, Funahashi T, et al. (2012) High circulating levels of S100A8/A9 complex (calprotectin) in male Japanese with abdominal adiposity and dysregulated expression of S100A8 and S100A9 in adipose tissues of obese mice. Biochem Biophys Res Commun 419: 782–789.
9. Mortensen OH, Nielsen AR, Erikstrup C, Plomgaard P, Fischer CP, et al. (2009) Calprotectin—a novel marker of obesity. PLoS One 4: e7419.
10. Matsuo S, Imai E, Horio M, Yasuda Y, Tomita K, et al. (2009) Revised equations for estimated GFR from serum creatinine in Japan. Am J Kidney Dis 53: 982–992.
11. Gross JL, de Azevedo MJ, Silveiro SP, Canani LH, Caramori ML, et al. (2005) Diabetic nephropathy: diagnosis, prevention, and treatment. Diabetes Care 28: 164–176.
12. Kambham N, Markowitz GS, Valeri AM, Lin J, D'Agati VD (2001) Obesity-related glomerulopathy: an emerging epidemic. Kidney Int 59: 1498–1509.
13. Praga M, Morales E (2006) Obesity, proteinuria and progression of renal failure. Curr Opin Nephrol Hypertens 15: 481–486.
14. Kawasaki Y, Hosoya M, Takahashi A, Isome M, Tanji M, et al. (2005) Myeloid-related protein 8 expression on macrophages is a useful prognostic marker for renal dysfunction in children with MPGN type 1. Am J Kidney Dis 45: 510–518.
15. Nishiyama A, Konishi Y, Ohashi N, Morikawa T, Urushihara M, et al. (2011) Urinary angiotensinogen reflects the activity of intrarenal renin-angiotensin system in patients with IgA nephropathy. Nephrol Dial Transplant 26: 170–177.
16. Ogawa Y, Mukoyama M, Yokoi H, Kasahara M, Mori K, et al. (2012) Natriuretic peptide receptor guanylyl cyclase-A protects podocytes from aldosterone-induced glomerular injury. J Am Soc Nephrol 23: 1198–1209.
17. Yokoi H, Mukoyama M, Mori K, Kasahara M, Suganami T, et al. (2008) Overexpression of connective tissue growth factor in podocytes worsens diabetic nephropathy in mice. Kidney Int 73: 446–455.
18. Hoshino K, Takeuchi O, Kawai T, Sanjo H, Ogawa T, et al. (1999) Cutting edge: Toll-like receptor 4 (TLR4)-deficient mice are hyporesponsive to lipopolysaccharide: evidence for TLR4 as the Lps gene product. J Immunol 162: 3749–3752.
19. Suganami T, Tanimoto-Koyama K, Nishida J, Itoh M, Yuan X, et al. (2007) Role of the Toll-like receptor 4/NF-kappaB pathway in saturated fatty acid-induced inflammatory changes in the interaction between adipocytes and macrophages. Arterioscler Thromb Vasc Biol 27: 84–91.
20. Pepper RJ, Hamour S, Chavele KM, Todd SK, Rasmussen N, et al. (2013) Leukocyte and serum S100A8/S100A9 expression reflects disease activity in ANCA-associated vasculitis and glomerulonephritis. Kidney Int 83: 1150–1158.
21. Ravid M, Brosh D, Ravid-Safran D, Levy Z, Rachmani R (1998) Main risk factors for nephropathy in type 2 diabetes mellitus are plasma cholesterol levels, mean blood pressure, and hyperglycemia. Arch Intern Med 158: 998–1004.
22. Adler AI, Stratton IM, Neil HA, Yudkin JS, Matthews DR, et al. (2000) Association of systolic blood pressure with macrovascular and microvascular complications of type 2 diabetes (UKPDS 36): prospective observational study. Bmj 321: 412–419.
23. Ruggenenti P, Remuzzi G (1998) Nephropathy of type-2 diabetes mellitus. J Am Soc Nephrol 9: 2157–2169.
24. Taft JL, Nolan CJ, Yeung SP, Hewitson TD, Martin FI (1994) Clinical and histological correlations of decline in renal function in diabetic patients with proteinuria. Diabetes 43: 1046–1051.
25. Matsusaka T, Niimura F, Shimizu A, Pastan I, Saito A, et al. (2012) Liver angiotensinogen is the primary source of renal angiotensin II. J Am Soc Nephrol 23: 1181–1189.
26. Kuwabara T, Mori K, Mukoyama M, Kasahara M, Yokoi H, et al. (2009) Urinary neutrophil gelatinase-associated lipocalin levels reflect damage to glomeruli, proximal tubules, and distal nephrons. Kidney Int 75: 285–294.
27. Kawasaki Y, Suyama K, Go H, Imamura T, Ushijima Y, et al. (2009) Accumulation of macrophages expressing myeloid-related protein 8 associated with the progression of sclerotic changes in children with IgA nephropathy. Tohoku J Exp Med 218: 49–55.
28. Nagareddy PR, Murphy AJ, Stirzaker RA, Hu Y, Yu S, et al. (2013) Hyperglycemia promotes myelopoiesis and impairs the resolution of atherosclerosis. Cell Metab 17: 695–708.
29. Jin Y, Sharma A, Carey C, Hopkins D, Wang X, et al. (2013) The Expression of Inflammatory Genes Is Upregulated in Peripheral Blood of Patients with Type 1 Diabetes. Diabetes Care.
30. Longo VD, Finch CE (2003) Evolutionary medicine: from dwarf model systems to healthy centenarians? Science 299: 1342–1346.

frontiers in
ENDOCRINOLOGY

MINI REVIEW ARTICLE
published: 26 September 2014
doi: 10.3389/fendo.2014.00152

The G-protein-coupled long-chain fatty acid receptor GPR40 and glucose metabolism

Tsutomu Tomita[1]*, Kiminori Hosoda[1], Junji Fujikura[1], Nobuya Inagaki[1] and Kazuwa Nakao[2]

[1] Department of Diabetes, Endocrinology and Nutrition, Kyoto University Graduate School of Medicine, Kyoto, Japan
[2] Medical Innovation Center, Kyoto University Graduate School of Medicine, Kyoto, Japan

Edited by:
Ikuo Kimura, Tokyo University of Agriculture and Technology, Japan

Reviewed by:
Carol Huang, University of Calgary, Canada
Kay Waud, Jones Institute for Reproductive Medicine, USA

***Correspondence:**
Tsutomu Tomita, Department of Diabetes, Endocrinology and Nutrition, Kyoto University Graduate School of Medicine, 54 Shogoin Kawaharacho, Sakyo, Kyoto 606-8507, Japan
e-mail: tt@kuhp.kyoto-u.ac.jp

Free fatty acids (FFAs) play a pivotal role in metabolic control and cell signaling processes in various tissues. In particular, FFAs are known to augment glucose-stimulated insulin secretion by pancreatic beta cells, where fatty acid-derived metabolites, such as long-chain fatty acyl-CoAs, are believed to act as crucial effectors. Recently, G-protein-coupled receptor 40 (GPR40), a receptor for long-chain fatty acids, was reported to be highly expressed in pancreatic beta cells and involved in the regulation of insulin secretion. Hence, GPR40 is considered to be a potential therapeutic target for the treatment of diabetes. In this review, we summarize the identification and gene expression patterns of GPR40 and its role in glucose metabolism. We also discuss the potential application of GPR40 as a therapeutic target.

Keywords: GPR40, FFAR1, LCFA, insulin secretion, pancreatic beta cells

INTRODUCTION

Free fatty acids (FFAs) are essential nutrients that also act as signaling molecules in various tissues. Long-chain fatty acids (LCFAs) play a role in the augmentation of glucose-stimulated insulin secretion (GSIS) (1). GSIS was observed to be considerably decreased by FFA depletion following *in vivo* administration of nicotinic acid to rats (2) and humans (3). Thus, FFA-mediated augmentation is considered to be physiologically significant. However, the underlying mechanisms of FFA-mediated augmentation of GSIS have not been fully elucidated. Several investigators have recently demonstrated that FFAs act as ligands for membrane-bound G-protein-coupled receptors (GPCRs) such as G-protein-coupled receptor 40 (GPR40), GPR41, GPR43, and GPR120. Among these, GPR40 is preferentially expressed by pancreatic beta cells in rodents and augments GSIS after acute exposure to LCFAs, highlighting the role of GPR40 as a potential key molecule in the regulation of insulin secretion.

LCFA RECEPTOR GPR40

GPR40 consists of 300 residues and was originally reported as an orphan GPCR (4). GPR40 was deorphaned by screening using a fluorometric imaging plate reader (FLIPR) system, which detects increases in Ca^{2+} concentrations in cultured cells with transiently expressed GPR40 cDNA (5, 6). GPR40 is reportedly activated by LCFAs (C12–22) and several eicosanoids in theoretically physiological concentration ranges. The profiles of putative GPR40 ligands are well conserved among mice, rats, and humans (5).

GPR40 GENE EXPRESSION IN RODENTS

Among rat tissues, GPR40 mRNA is almost exclusively expressed in the pancreas. In pancreatic islets, GPR40 mRNA levels were found to be approximately 17-fold higher than the levels in the pancreas, suggesting selective GPR40 expression by pancreatic islets. Considerable amounts of GPR40 mRNA were detected in the pancreatic beta cell lines MIN6, betaTC-3, HIT-T15, and Rin5F but not in the pancreatic alpha cell line alphaTC1. Furthermore, *in situ* hybridization with rat pancreatic islets suggested that GPR40 mRNA is preferentially expressed in pancreatic beta cells (5).

Reports using anti-GPR40 antibodies suggest that GPR40 protein is also probably preferentially expressed in pancreatic islets (7, 8).

ROLES OF GPR40 IN REGULATION OF INSULIN SECRETION

In MIN6 cells, insulin secretion was augmented by LCFAs in a dose-dependent manner, and the augmentation was observed only under hyperglycemic conditions (11–22 mM) (5), indicating the LCFA-mediated augmentation of insulin secretion is glucose-dependent. Silencing of GPR40 gene expression using siRNA almost abolished the augmentation effects of LCFAs, indicating that GPR40 is involved in LCFA-mediated regulation of insulin secretion. GPR40 is a class A GPCR, highlighting the potential of GPR40 as a target for novel anti-diabetic oral drugs with low risk of hypoglycemia, considering that LCFA-mediated augmentation of insulin secretion is glucose-dependent.

GPR40 GENE EXPRESSION IN HUMANS

Although GPR40 is reportedly preferentially expressed by pancreatic beta cells in both rats and mice, little is known about GPR40 gene expression in humans. In this context, we assessed GPR40 mRNA expression in fresh human tissues obtained during surgery (9, 10). Analysis of 12 specimens of non-tumor pancreatic tissues revealed a considerable amount of GPR40 mRNA in each. In three pancreatic islet tissues specimens, GPR40 mRNA levels were approximately 20-fold higher than those in pancreatic tissues, comparable to the levels of sulfonylurea receptor 1, which is

known to be highly expressed in pancreatic beta cells. High levels of GPR40 mRNA were detected in insulinoma (beta cell tumor) tissues in three cases; in contrast, GPR40 mRNA was undetectable in glucagonoma (alpha cell tumor) tissues (10, 11). In human pancreas, GPR40 mRNA level is positively and significantly correlated with the insulinogenic index, an index reflecting the function of pancreatic beta cells. These results indicate that GPR40 is highly expressed in human pancreatic beta cells and possibly involved in the positive regulation of insulin secretion (10).

REGULATION OF GPR40 GENE EXPRESSION

Though the mechanisms underlying the regulation of GPR40 gene expression is not fully understood, possible mechanisms include the PDX-1/IPF1 (12), which reportedly binds to the promoter region of the GPR40 gene (13). Moreover, nutrients and therapeutic drugs such as glucose (12), palmitate, and rosiglitazone (8) are reportedly involved in the regulation of GPR40 gene expressions.

THERAPEUTIC IMPLICATIONS OF GPR40

Although an initial report of systemic GPR40 knockout (KO) mice and beta cell-specific GPR40 transgenic (Tg) mice using the PDX-1/IPF1 promoter suggested possible involvement of GPR40 in insulin resistance in the liver and beta cell failure (14), later reports using GPR40 KO mice found no link between GPR40 and beta cell dysfunction (15, 16). Studies using GPR40 KO mice suggest the implication of GPR40 in the regulation of insulin secretion, at least under some conditions including loading of intralipid (17), high-fat diet (15), hyperglycemic glucose clamp, and arginine (18). Furthermore, GPR40 Tg mice with the mouse INS2 promoter exhibited better glucose tolerance with enhanced GSIS (19), suggesting therapeutic implications of GPR40 rather than a gateway of beta cell toxicity.

Additionally, recent reports suggest that GPR40 is expressed in enteroendocrine cells and involved in the positive regulation of intestinal hormones including glucagon-like peptide-1 (GLP-1), glucose-dependent insulinotropic polypeptide (GIP), and cholecystokinin (20–22).

GPR40 AGONISTS AS ANTI-DIABETIC DRUGS

Recently, TAK-875 (Fasiglifam), a novel GPR40 selective agonist (23), was reported as a potential oral anti-diabetic drug. The potency of TAK-875 is approximately 400-fold greater than that of the endogenous ligand oleic acid (24), and it does not activate GPR120 (23), another GPCR for LCFAs. TAK-875 augmented insulin secretion under high-glucose conditions in the rat pancreatic beta cell line INS1 833/14 (24) and human pancreatic islets (25) but did not affect glucagon secretion in humans (25), in accordance with the observations in humans by our group and others (9–11). TAK-875 significantly improved glycemic control with the augmentation of insulin secretion in diabetic rat models such as Wistar fatty rats (23) and Zucker diabetic fatty rats (24).

In phase 2, randomized, double-blind, placebo-controlled trial in patients with type 2 diabetes, HbA1c was decreased in a dose-dependent manner in TAK-875 groups, and the HbA1c-lowering effect (50–200 mg, approximately −1.1% in 12 weeks) was comparable to that in glimepiride (4 mg) group, while the incidence of hypoglycemia in TAK-875 was similar to the placebo group and markedly lower than the glimepiride group (26). In Japanese patients with type 2 diabetes, 12-week treatment with TAK-875 also decreased HbA1c levels in a dose-dependent manner, and the HbA1c-lowering effect (50–200 mg, approximately −1.3%) was comparable to that in the glimepiride (1 mg) group (27).

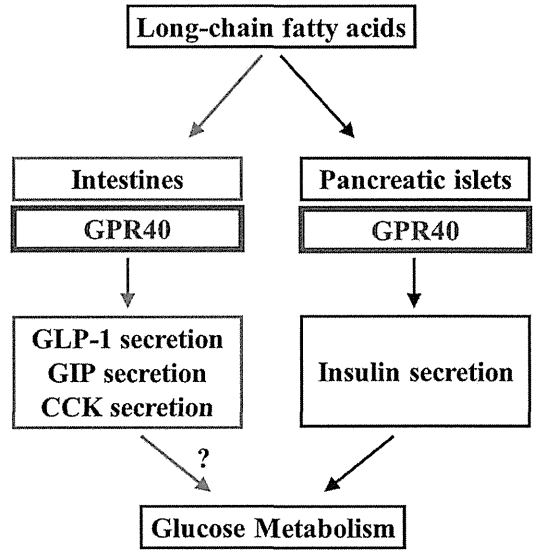

FIGURE 1 | LCFAs augment insulin secretion by stimulating GPR40 in beta cells in the pancreas. GPR40 is also reportedly involved in the positive regulation of secretion of some intestinal hormones. Studies using GPR40 agonists and analyses of beta cell-specific GPR40 transgenic mice indicate that GPR40 is involved in the regulation of glucose metabolism, at least by the augmentation of insulin secretion. Because LCFA-mediated augmentation of insulin secretion is glucose-dependent, GPR40 is thought to be a potential target for novel anti-diabetic drugs with low risk of hypoglycemia.

Though TAK-875 seemed to be a promising anti-diabetic drug, regrettably, its development was terminated in 2013 because of the risk of possible liver damage. Although the cause of the liver damage remains unclear, GPR40 is not expressed in the human liver (6, 10), suggesting that the toxicity may not be due to the GPR40 receptor itself but chemical characteristic of TAK-875 or its dose used in the clinical trials. Still, several GPR40 agonists continue to be evaluated in both preclinical (Bristol-Myers Squibb, Merck, Amgen, Johnson & Johnson, Astellas, Daiichi Sankyo, Piramal, and Connexios) and clinical (Japan Tobacco) trials, and the further development is expected in the study elucidating the significance of GPR40 in glucose and other metabolism.

CONCLUSION

Incretin mimetic-type drugs have been implicated in GPCR-mediated regulation of insulin secretion in diabetes. GPR40 is a GPCR that is highly expressed in pancreatic beta cells and involved in insulin secretion in rodents and humans. Hence, GPR40 is a potential therapeutic target in diabetes, which can lead to the development of oral drugs with fewer hypoglycemic side effects. Furthermore, GPR40 is reportedly implicated in the regulation of incretin secretion from enteroendocrine cells. GPR40 may be important to unveil the link between FFA signaling and beta

cell function as well as glucose metabolism (**Figure 1**). Hence, further studies are warranted to elucidate the physiological and pathophysiological implications of GPR40.

REFERENCES

1. Stein DT, Esser V, Stevenson BE, Lane KE, Whiteside JH, Daniels MB, et al. Essentiality of circulating fatty acids for glucose-stimulated insulin secretion in the fasted rat. *J Clin Invest* (1996) **97**:2728–35. doi:10.1172/JCI118727
2. Dobbins RL, Chester MW, Stevenson BE, Daniels MB, Stein DT, McGarry JD. A fatty acid-dependent step is critically important for both glucose- and non-glucose-stimulated insulin secretion. *J Clin Invest* (1998) **101**:2370–6. doi:10.1172/JCI1813
3. Dobbins RL, Chester MW, Daniels MB, McGarry JD, Stein DT. Circulating fatty acids are essential for efficient glucose-stimulated insulin secretion after prolonged fasting in humans. *Diabetes* (1998) **47**:1613–8. doi:10.2337/diabetes.47.10.1613
4. Takeda S, Kadowaki S, Haga T, Takaesu H, Mitaku S. Identification of G protein-coupled receptor genes from the human genome sequence. *FEBS Lett* (2002) **520**:97–101. doi:10.1016/S0014-5793(02)02775-8
5. Itoh Y, Kawamata Y, Harada M, Kobayashi M, Fujii R, Fukusumi S, et al. Free fatty acids regulate insulin secretion from pancreatic beta cells through GPR40. *Nature* (2003) **422**:173–6. doi:10.1038/nature01478
6. Briscoe CP, Tadayyon M, Andrews JL, Benson WG, Chambers JK, Eilert MM, et al. The orphan G protein-coupled receptor GPR40 is activated by medium and long chain fatty acids. *J Biol Chem* (2003) **278**:11303–11. doi:10.1074/jbc.M211495200
7. Hirasawa A, Itsubo C, Sadakane K, Hara T, Shinagawa S, Koga H, et al. Production and characterization of a monoclonal antibody against GPR40 (FFAR1; free fatty acid receptor 1). *Biochem Biophys Res Commun* (2008) **365**:22–8. doi:10.1016/j.bbrc.2007.10.142
8. Meidute Abaraviciene S, Muhammed SJ, Amisten S, Lundquist I, Salehi A. GPR40 protein levels are crucial to the regulation of stimulated hormone secretion in pancreatic islets. Lessons from spontaneous obesity-prone and non-obese type 2 diabetes in rats. *Mol Cell Endocrinol* (2013) **381**:150–9. doi:10.1016/j.mce.2013.07.025
9. Tomita T, Masuzaki H, Noguchi M, Iwakura H, Fujikura J, Tanaka T, et al. GPR40 gene expression in human pancreas and insulinoma. *Biochem Biophys Res Commun* (2005) **338**:1788–90. doi:10.1016/j.bbrc.2005.10.161
10. Tomita T, Masuzaki H, Iwakura H, Fujikura J, Noguchi M, Tanaka T, et al. Expression of the gene for a membrane-bound fatty acid receptor in the pancreas and islet cell tumours in humans: evidence for GPR40 expression in pancreatic beta cells and implications for insulin secretion. *Diabetologia* (2006) **49**:962–8. doi:10.1007/s00125-006-0193-8
11. Odori S, Hosoda K, Tomita T, Fujikura J, Kusakabe T, Kawaguchi Y, et al. GPR119 expression in normal human tissues and islet cell tumors: evidence for its islet-gastrointestinal distribution, expression in pancreatic beta and alpha cells, and involvement in islet function. *Metabolism* (2013) **62**:70–8. doi:10.1016/j.metabol.2012.06.010
12. Kebede M, Ferdaoussi M, Mancini A, Alquier T, Kulkarni RN, Walker MD, et al. Glucose activates free fatty acid receptor 1 gene transcription via phosphatidylinositol-3-kinase-dependent O-GlcNAcylation of pancreas-duodenum homeobox-1. *Proc Natl Acad Sci U S A* (2012) **109**:2376–81. doi:10.1073/pnas.1114350109
13. Bartoov-Shifman R, Ridner G, Bahar K, Rubins N, Walker MD. Regulation of the gene encoding GPR40, a fatty acid receptor expressed selectively in pancreatic beta cells. *J Biol Chem* (2007) **282**:23561–71. doi:10.1074/jbc.M702115200
14. Steneberg P, Rubins N, Bartoov-Shifman R, Walker MD, Edlund H. The FFA receptor GPR40 links hyperinsulinemia, hepatic steatosis, and impaired glucose homeostasis in mouse. *Cell Metab* (2005) **1**:245–58. doi:10.1016/j.cmet.2005.03.007
15. Kebede M, Alquier T, Latour MG, Semache M, Tremblay C, Poitout V. The fatty acid receptor GPR40 plays a role in insulin secretion in vivo after high-fat feeding. *Diabetes* (2008) **57**:2432–7. doi:10.2337/db08-0553
16. Lan H, Hoos LM, Liu L, Tetzloff G, Hu W, Abbondanzo SJ, et al. Lack of FFAR1/GPR40 does not protect mice from high-fat diet-induced metabolic disease. *Diabetes* (2008) **57**:2999–3006. doi:10.2337/db08-0596
17. Latour MG, Alquier T, Oseid E, Tremblay C, Jetton TL, Luo J, et al. GPR40 is necessary but not sufficient for fatty acid stimulation of insulin secretion in vivo. *Diabetes* (2007) **56**:1087–94. doi:10.2337/db06-1532
18. Alquier T, Peyot ML, Latour MG, Kebede M, Sorensen CM, Gesta S, et al. Deletion of GPR40 impairs glucose-induced insulin secretion in vivo in mice without affecting intracellular fuel metabolism in islets. *Diabetes* (2009) **58**:2607–15. doi:10.2337/db09-0362
19. Nagasumi K, Esaki R, Iwachidow K, Yasuhara Y, Ogi K, Tanaka H, et al. Overexpression of gpr40 in pancreatic β-cells augments glucose stimulated insulin secretion and improves glucose tolerance in normal and diabetic mice. *Diabetes* (2009) **58**:1067–76. doi:10.2337/db08-1233
20. Edfalk S, Steneberg P, Edlund H. Gpr40 is expressed in enteroendocrine cells and mediates free fatty acid stimulation of incretin secretion. *Diabetes* (2008) **57**:2280–7. doi:10.2337/db08-0307
21. Parker HE, Habib AM, Rogers GJ, Gribble FM, Reimann F. Nutrient-dependent secretion of glucose-dependent insulinotropic polypeptide from primary murine K cells. *Diabetologia* (2009) **52**:289–98. doi:10.1007/s00125-008-1202-x
22. Liou AP, Lu X, Sei Y, Zhao X, Pechhold S, Carrero RJ, et al. The G-protein-coupled receptor GPR40 directly mediates long-chain fatty acid-induced secretion of cholecystokinin. *Gastroenterology* (2011) **140**:903–12. doi:10.1053/j.gastro.2010.10.012
23. Negoro N, Sasaki S, Mikami S, Ito M, Suzuki M, Tsujihata Y, et al. Discovery of TAK-875: a potent, selective, and orally bioavailable GPR40 agonist. *ACS Med Chem Lett* (2010) **1**:290–4. doi:10.1021/ml1000855
24. Tsujihata Y, Ito R, Suzuki M, Harada A, Negoro N, Yasuma T, et al. TAK-875, an orally available G protein-coupled receptor 40/free fatty acid receptor 1 agonist, enhances glucose-dependent insulin secretion and improves both postprandial and fasting hyperglycemia in type 2 diabetic rats. *J Pharmacol Exp Ther* (2011) **339**:228–37. doi:10.1124/jpet.111.183772
25. Yashiro H, Tsujihata Y, Takeuchi K, Hazama M, Johnson PR, Rorsman P. The effects of TAK-875, a selective G protein-coupled receptor 40/free fatty acid 1 agonist, on insulin and glucagon secretion in isolated rat and human islets. *J Pharmacol Exp Ther* (2012) **340**:483–9. doi:10.1124/jpet.111.187708
26. Burant CF, Viswanathan P, Marcinak J, Cao C, Vakilynejad M, Xie B, et al. TAK-875 versus placebo or glimepiride in type 2 diabetes mellitus: a phase 2, randomised, double-blind, placebo-controlled trial. *Lancet* (2012) **379**:1403–11. doi:10.1016/S0140-6736(11)61879-5
27. Kaku K, Araki T, Yoshinaka R. Randomized, double-blind, dose-ranging study of TAK-875, a novel GPR40 agonist, in Japanese patients with inadequately controlled type 2 diabetes. *Diabetes Care* (2013) **36**:245–50. doi:10.2337/dc12-0872

Conflict of Interest Statement: The authors declare that the research was conducted in the absence of any commercial or financial relationships that could be construed as a potential conflict of interest.

Received: 12 June 2014; accepted: 12 September 2014; published online: 26 September 2014.

Citation: Tomita T, Hosoda K, Fujikura J, Inagaki N and Nakao K (2014) The G-protein-coupled long-chain fatty acid receptor GPR40 and glucose metabolism. Front. Endocrinol. 5:152. doi: 10.3389/fendo.2014.00152

This article was submitted to Diabetes, a section of the journal Frontiers in Endocrinology.

Clin Exp Nephrol (2015) 19:99–106
DOI 10.1007/s10157-014-0952-7

ORIGINAL ARTICLE

An AKI biomarker lipocalin 2 in the blood derives from the kidney in renal injury but from neutrophils in normal and infected conditions

Junya Kanda · Kiyoshi Mori · Hiroshi Kawabata · Takashige Kuwabara · Keita P. Mori · Hirotaka Imamaki · Masato Kasahara · Hideki Yokoi · Chisaki Mizumoto · Nils H. Thoennissen · H. Phillip Koeffler · Jonathan Barasch · Akifumi Takaori-Kondo · Masashi Mukoyama · Kazuwa Nakao

Received: 3 August 2012 / Accepted: 17 February 2014 / Published online: 6 March 2014

Abstract

Background Lipocalin 2 (LCN2 or neutrophil gelatinase-associated lipocalin) is a secretory protein discovered from neutrophils, which accumulates in the blood and urine during acute kidney injury (AKI) and in the blood by bacterial infection. Little is known about the tissue source and molecular forms of this protein under normal and pathophysiologic conditions.

Methods By sandwich ELISA, serum and urinary LCN2 levels were measured in 36 patients with hematologic malignancies who transiently became neutropenic by stem cell transplantation (SCT). To evaluate contribution of neutrophil-derived LCN2 in the physiologic blood LCN2 concentrations, we examined CCAAT/enhancer-binding protein ε (C/EBPε) knockout mice, which lack mature neutrophils.

Results In patients without AKI and bacterial infection, at 1 week after SCT, the median blood neutrophil counts became zero and serum LCN2 levels were decreased by 76 ± 6 % ($p < 0.01$), but urinary LCN2 levels were not altered. During neutropenic conditions, bacterial infection caused only a modest rise of serum LCN2 but AKI produced a marked rise of serum and urinary LCN2 levels. Serum LCN2 concentrations in C/EBPε knockout mice were reduced by 66 ± 11 % compared to wild-type mice ($p < 0.05$). Blood LCN2 existed predominantly in high molecular weight forms (>100 kDa), while urinary LCN2 was mainly in low molecular weight forms.

Conclusion Our findings suggest that neutrophils are the major source of circulating LCN2 in normal and infected conditions, whereas blood and urinary LCN2 mainly derive from the kidney during AKI, and that the molecular forms and regulation of blood and urinary LCN2 are clearly distinct.

Keywords Acute kidney injury · Neutrophil · Sepsis, bone marrow transplantation · Biomarker

Electronic supplementary material The online version of this article (doi:10.1007/s10157-014-0952-7) contains supplementary material, which is available to authorized users.

J. Kanda · H. Kawabata · C. Mizumoto · A. Takaori-Kondo
Department of Hematology and Oncology, Graduate School of Medicine, Kyoto University, Kyoto, Japan

K. Mori (✉) · T. Kuwabara · K. P. Mori · H. Imamaki · M. Kasahara · H. Yokoi · M. Mukoyama · K. Nakao
Department of Medicine and Clinical Science, Kyoto University Graduate School of Medicine, 54 Shogoin Kawahara-cho, Sakyoku, Kyoto 606-8507, Japan
e-mail: keyem@kuhp.kyoto-u.ac.jp

N. H. Thoennissen · H. P. Koeffler
Division of Hematology and Oncology, Cedars-Sinai Medical Center, UCLA School of Medicine, Los Angeles, CA, USA

J. Barasch
Department of Medicine, Physicians and Surgeons of Columbia University, New York, NY, USA

Introduction

Lipocalin 2 (LCN2 or neutrophil gelatinase-associated lipocalin) was originally purified from activated neutrophils [1, 2]. LCN2 gene expression is detected not only in neutrophils, but also in various normal tissues, such as lung, liver, and adipose tissue [2–4]. Its expression is markedly upregulated by renal injury [5–8] and bacterial infection [9]. LCN2 is now known to exert a broad spectrum of biological activities including host defense [9], kidney differentiation [10] and modulation of organ damage [5].

Blood and urinary levels of LCN2 have been extensively studied as very promising biomarkers for an early diagnosis

of acute kidney injury (AKI) [2, 6, 7] and for monitoring of chronic kidney disease severity [11, 12], which may revolutionize our clinical practice in the near future. Bacterial infection also causes mild elevation of blood LCN2 levels [13, 14]. Thus, neutrophils and injured kidneys are two major candidate sites of LCN2 release in diseased conditions. Therefore, to make clinical judgment based upon LCN2 levels in the blood or urine, it is important to understand tissue source of LCN2. Furthermore, a fraction of neutrophil-derived LCN2 is covalently bound to gelatinase B (or metalloproteinase-9) [15, 16], but the details about the molecular forms of LCN2 in body fluid largely remain unknown.

In the present study, we examined whether neutrophils contribute to blood LCN2 levels in AKI or in bacterial infection by analyzing a unique subset of patients who were neutropenic after stem cell transplantation (SCT) [17]. Since not all cases were in complete remission status before SCT, we also studied wild-type and CCAAT/enhancer-binding protein ε (C/EBPε) knockout mice [18], which reflect normal and neutropenic conditions, respectively, in the absence of hematologic malignancies. To study the mode of existence of LCN2, we separated serum and urine with 100-kDa cutoff ultrafiltration membranes and measured the levels of high and low molecular weight (HMW and LMW) LCN2 forms. Furthermore, we examined LCN2/gelatinase B complex.

Methods

Patients

Patients with hematologic malignancies undergoing autologous or allogeneic SCTs at Kyoto University Hospital (Electronic Supplementary Material Table S1), healthy subjects and patients with renal disorders were enrolled under written informed consent. This prospective, observational study was approved by the ethical committee on human research of Kyoto University Graduate School of Medicine (approval number E-541). AKI was defined by $\geq$50 % elevation of serum creatinine level during the observation period in comparison with the level before SCT. Bacterial infection was determined by development of pyrexia (>38 °C) together with either a positive blood culture test or clinical symptoms highly suggestive of local infection or septic shock.

Animals

All animal experiments and protocols were approved by our institutional animal care and use committee. Sera were collected from C/EBPε$^{-/-}$, C/EBPε$^{+/-}$ mice and their wild-type littermates in a mixed background of 129SV × NIH Black Swiss at 8–10 weeks of age [18].

Expression vectors and promoter–reporter gene constructs

The human CCAAT/enhancer-binding protein (C/EBP) α cDNA [19] and the human C/EBPε32 cDNA [20] were sub-cloned into pCDNA3.1+ (Invitrogen, Carlsbad, CA). A luciferase reporter construct was prepared in pGL3 basic vector (Promega, Madison, WI), containing sequences between nucleotide positions −900 to +51 of human LCN2 promoter region [4].

Reporter assay

In 12-well plates, 1 × 10^5 293T cells were seeded per well 1 day before transfection. Either C/EBPα, C/EBPε32 or mock vector (pcDNA3.1+) was transfected into 293T cells with the reporter vector using TransFectin Lipid Reagent (BioRad, Hercules, CA). Forty-eight hours later, cell lysate was collected and measured for luciferase activity using Dual Luciferase Assay System (Promega, Madison, WI).

Elisa

Human and murine LCN2 concentrations in the serum or urine were determined once a week by sandwich ELISA (kits 036 and 042, BioPorto, Gentofte, Denmark). To separate serum and urine by molecular weights, samples were passed through 100-kDa cutoff filter (Amicon YM-100; Millipore Corp., Billerica, MA). LCN2/gelatinase B complex levels from humans were measured by ELISA (Quantikine, R&D Systems, Minneapolis, MN).

Western blot analysis

YM-100 flow through of mouse serum was separated by SDS-polyacrylamide gel electrophoresis, transferred onto polyvinylidene difluoride membranes, incubated with goat anti-mouse LCN2 antibody (R&D Systems, Minneapolis, MN), with peroxidase-conjugated anti-goat antibody, and detection was carried out using chemiluminescence. As standards, recombinant mouse LCN2 protein synthesized in BL21 bacteria was loaded [5].

Statistical analysis

Values are expressed as mean ± SEM, or median (interquartile range) when appropriate. Differences between repeated measures were assessed by one-way ANOVA with Bonferroni's post test. Comparison between two groups was carried out by unpaired Student's *t* test. The correlation

between blood neutrophil counts and LCN2 levels was tested by Pearson's correlation coefficient. Cross-sectional time series regression model was used in univariate and multivariate analyses to evaluate potential factors which were associated with the level of LCN2. Confounders that were analyzed included the number of neutrophils, lymphocytes and platelets, the levels of hemoglobin, serum creatinine, C-reactive protein, and body mass index (defined as body weight divided by square of height), and weeks after SCT. Significant independent variables in univariate analysis, as well as weeks, were included in multivariate analysis. Standardized coefficients were calculated to evaluate which of the independent variables have greater effects on the dependent variable. p values of <0.05 were considered statistically significant. All statistical analyses were performed using Stata software version 11 (Stata Corp., College Station, Texas, USA).

Table 1 Categorization of patients who underwent SCT

Group	Bact infect	AKI	Number	Peak sCRP (mg/dl)	Peak sCr (mg/dl)
1	−	−	12	0.8 (0.3–4.4)	0.8 (0.6–1.1)
2	+	−	12	7.0 (2.8–11.1)*	0.8 (0.6–0.9)
3	−	+	2	3.0 [1.0–4.9]#	2.4 [1.0–3.7]#
4	+	+	10	17.1 (5.4–24.9)*	2.3 (1.0–3.4)*

Bact infect bacterial infection, *AKI* acute kidney injury, *Peak* peak value during observation period (which is within 4 weeks after SCT), *sCRP* serum C-reactive protein, *sCr* serum creatinine

Values are median (interquartile range), or mean [range]

* $p < 0.05$ vs. Group 1

Results

Blood and urine human LCN2 levels in patients undergoing stem cell transplantation

We studied 36 patients who underwent SCT for their hematological malignancies. The time course of serum and urinary LCN2 levels during periods from pre-transplantation (between −2 and −1 weeks) to 4 weeks after autologous or allogeneic SCT were examined (Fig. S1). These patients were categorized into 4 groups based on the presence or absence of AKI or bacterial infection (Table 1). Twelve patients (33 %) were categorized as Group 1 [bacterial infection (−), AKI (−)]. At 1 week, median blood neutrophil count became 0/μl, and serum LCN2 level was reduced by 76 ± 6 % (from 63 ± 15 to 10 ± 1 ng/ml, $p < 0.01$, Fig. 1). Among the 4 groups, the general trend of neutrophil counts and serum LCN2 concentrations during the observation period was similar, with the lowest levels at 1 and 2 weeks and gradual recovery towards 4 weeks (Figs. 1, 2). These findings suggest that the predominant source of circulating LCN2 is blood neutrophils but substantial amount of a non-neutrophil pool also exists.

Twelve subjects (33 %) were categorized as Group 2 [bacterial infection (+), AKI (−)] (Fig. 1). Bacterial infection was diagnosed on day 8.2 ± 1.7 (Fig. S1). Peak serum C-reactive protein (CRP) levels were 8.8-fold higher in Group 2 as compared to Group 1 ($p < 0.05$, Table 1). The time course of blood neutrophil counts and serum LCN2 levels was roughly similar as compared to Group 1, but neutrophil counts were significantly higher at 3 weeks in Group 2 ($p < 0.05$, Fig. 1). In Group 2, 6 patients had

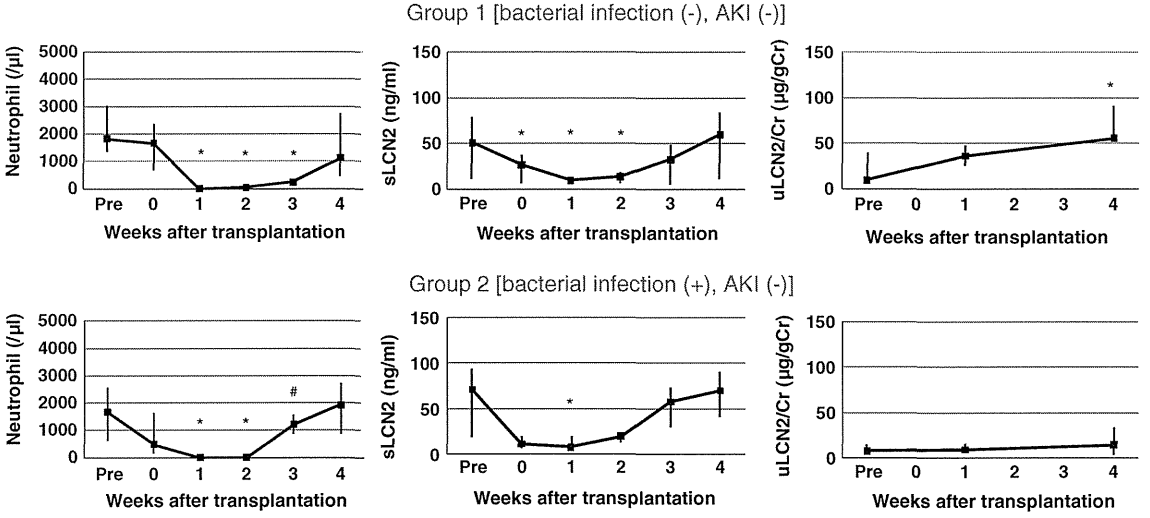

Fig. 1 Changes of blood neutrophil counts, serum and urinary LCN2 levels in Groups 1 and 2. Serum and urine (s, u) LCN2 levels and blood neutrophil counts are expressed as median (interquartile range). *AKI* acute kidney injury. *$p < 0.05$ vs. pre-transplantation (pre); #$p < 0.05$ vs. Group 1 at 3 weeks

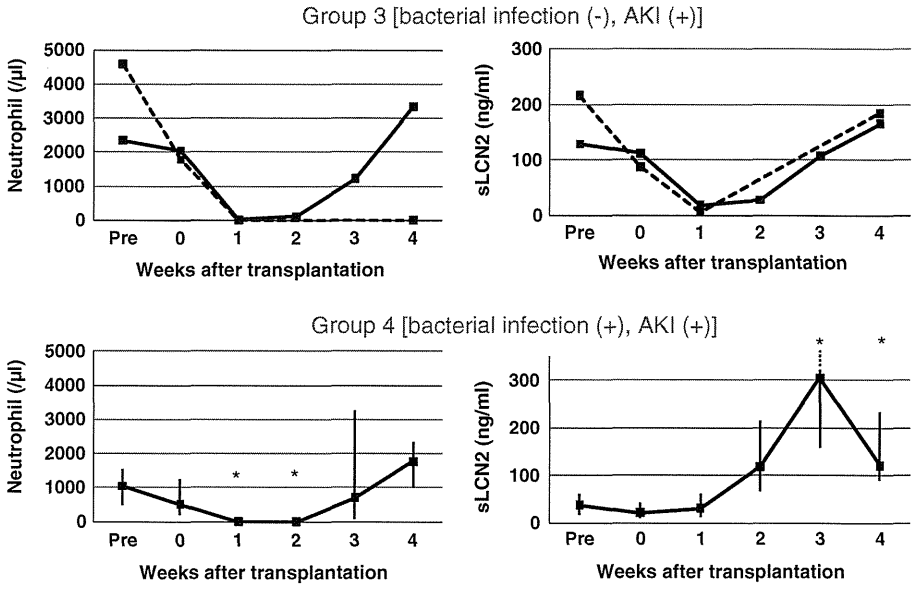

Fig. 2 Changes of blood neutrophil counts and serum LCN2 levels in Groups 3 and 4. Serum (s) LCN2 levels and neutrophil counts are expressed as median (interquartile range) for Group 4. For Group 3, values of two subjects are shown separately. Urinary LCN2 concentrations were highly variable among cases in Groups 3 and 4, and are not presented here (see online supplementary Fig. S2). sLCN2 in Group 4 at 3 weeks was 305 (147–1074) ng/ml and the top *error bar* for interquartile range was larger than what is shown in this figure (as indicated in *dotted line*). *$p < 0.05$ vs. pre-transplantation (pre)

zero neutrophil counts not only at 1 week but also at 2 weeks and developed bacterial infection on day 8.2 ± 1.4. Their serum LCN2 levels at 1 and 2 weeks were 12 ± 4 and 25 ± 9 ng/ml, respectively. These findings suggest that bacterial infection caused small amount of LCN2 release from non-myeloid tissues, which could be from the lung, liver, spleen or adipose tissue [2–4]. The urinary LCN2 excretion in Groups 1 and 2, unlike serum LCN2 levels, did not decrease during the first week (which was neutrophil-depleted period), indicating that circulating and urinary LCN2 levels were regulated in distinct manners (Fig. 1).

Most patients with AKI also suffered from bacterial infection, and only 2 patients (6 %) belonged to Group 3 [bacterial infection (−), AKI (+)] (Fig. 2). These 2 patients developed AKI at 3 and 4 weeks, respectively, and their serum LCN2 levels at 4 weeks tended to be higher compared to patients without AKI (Groups 1 and 2), but the sample number in Group 3 was too small for statistical analysis.

Ten patients (28 %) were classified into Group 4 [bacterial infection (+), AKI (+)]. The peak serum creatinine levels were 2.9-fold higher in Group 4 compared to Group 1 ($p < 0.05$, Table 1). Diagnoses of bacterial infection and AKI were made on days 6.9 ± 1.2 and 8.3 ± 1.4, respectively. Blood neutrophil counts became almost zero at 1 and 2 weeks as similar to the cases in Groups 1–3. However, during this nadir period especially at 2 weeks, serum LCN2 levels became much higher than the levels before SCT (Fig. 2; Fig. S1). Three patients in Group 4 and one in Group 3 started to receive continuous hemodiafiltration (CHDF) at various time points due to oliguria or hyperkalemia (Fig. S2). The timing of CHDF initiation was closely associated with elevation in the serum and urinary LCN2 levels by log orders of magnitude, occasionally reaching the levels above 300 ng/ml or 2,000 μg/gCr, respectively. These cases clearly show that AKI causes a steep elevation in serum and urinary LCN2 levels, even in the absence of neutrophils.

Determinants of serum LCN2 levels

We identified a strong positive correlation between neutrophil counts and serum LCN2 levels among samples excluding those collected when AKI was present (Fig. 3). Blood samples during AKI contained larger amounts of LCN2 than ones with no AKI. Multivariate analyses for all samples (with and without AKI) showed that the serum levels of LCN2 were significantly associated with neutrophil counts (standardized coefficient 0.57, $p < 0.001$) as well as with serum CRP levels (standardized coefficient 0.16, $p < 0.05$, Table 2). The significant positive correlation between serum LCN2 and creatinine levels in univariate analysis was lost in multivariate analysis, likely because samples with elevated serum creatinine levels were partially enriched in those with low blood neutrophil counts (Figs. S1, S2).

Characterization of molecular forms of blood and urine LCN2

LCN2 protein in serum or urine may exist in several molecular forms, including a 25-kDa monomer, a 46-kDa homodimer and a 135-kDa heterodimer with gelatinase B (or MMP-9) [1, 16]. Serum and urine were passed through 100-kDa cutoff membrane to separate LCN2 into HMW

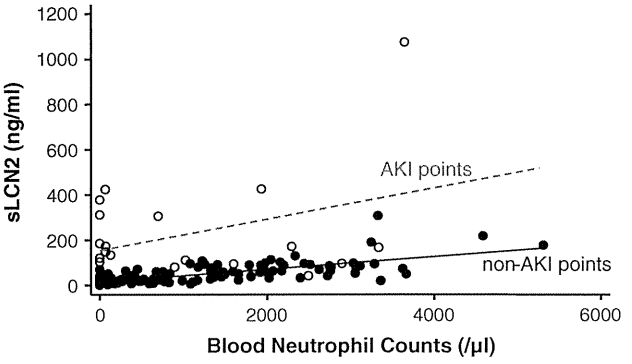

Fig. 3 Correlation of blood neutrophil counts and serum LCN2 levels. *Closed circles* and a *solid line*, non-AKI points and their regression line ($r = 0.73$, $p < 0.001$); *open circles* and a *dotted line*, AKI points and their regression line ($r = 0.35$, $p = 0.12$)

Table 2 Correlation of serum LCN2 levels with clinical parameters

Independent variables	Univariate		Multivariate	
	Standardized coefficient	*p*	Standardized coefficient	*p*
Neutrophil counts	0.570	<0.001	0.574	<0.001
Lymphocyte counts	−0.146	0.064		
Platelet counts	−0.049	0.525		
Hemoglobin	0.003	0.970		
Creatinine	0.217	0.005	0.100	0.160
CRP	0.233	0.002	0.159	0.031
BMI	0.190	0.093		

CRP C-reactive protein, *BMI* body mass index

and LMW forms (Fig. S3). Approximately 82 % of serum LCN2 existed as HMW form, and presence of neither bacterial infection nor AKI affected the ratios (Fig. 4; Fig. S3). On the other hand, approximately 99 % of urinary LCN2 was in LMW form in most patients who underwent SCT (both before and after SCT) and in healthy subjects (data not shown). Exclusively, urine from SCT patients who developed AKI with overt proteinuria (urinary protein level >1 g/g creatinine) contained as much as 37 % of HMW form. Similarly, patients with nephrotic range proteinuria due to chronic kidney disease had large amount of HMW LCN2 in the urine (Fig. 4). These findings suggest that, if glomerular size barrier is functioning normally, only a small fraction of HMW LCN2 in the blood (as is the case with 60-kDa albumin) is filtered through glomeruli and trace amount, if any, is excreted into urine. Thus, circulating LCN2, due to its large molecular size, likely has a much longer blood half-life than that of LCN2 monomer (which is about 10 min) [21].

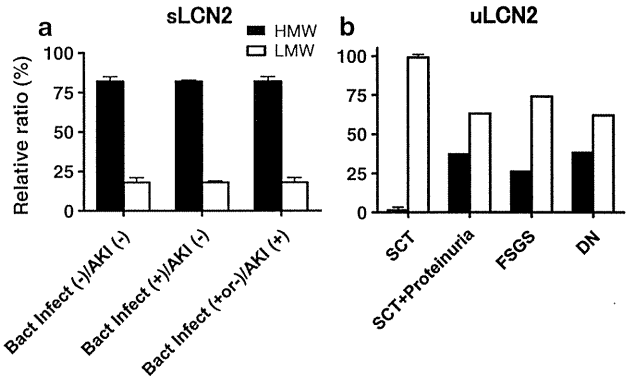

Fig. 4 Relative ratios of high and low molecular weight LCN2 in the serum and urine. **a** Serum LCN2 (sLCN2) levels. Values are mean ± SEM. $n = 10$, 4 and 5 from the left. **b** Urinary LCN2 (uLCN2) levels. SCT, patients undergoing stem cell transplantation who either had or did not have AKI ($n = 2$ each, mean of 4 is shown). SCT + Proteinuria, SCT patients who developed AKI with overt proteinuria (>1 g/g creatinine, mean of $n = 2$ is shown). Cases of focal segmental glomerulosclerosis (FSGS; $n = 1$) and diabetic nephropathy (DN; mean of $n = 2$) who had overt proteinuria are also shown. Their clinical data are available in online suppl. Fig. 3

A portion of LCN2 secreted from neutrophils is covalently bound to gelatinase B [15, 16] and LCN2/gelatinase B complex is one of the candidate forms of HMW LCN2. We examined the content of this complex in the serum and urine (Table S2). Ratio of complex among total LCN2 immunoreactivity was <30 % in serum of healthy subjects and patients undergoing SCT. Furthermore, the concentration of complex in urine was quite low (<2 ng/ml, and typically <3 % of total urine LCN2 immunoreactivity). These findings suggest that the majority of HMW LCN2 in the blood exists in forms other than LCN2/gelatinase B complex. Furthermore, the ratio of complex in the blood was largely and temporarily reduced when patients were in neutropenic periods (at 1 week after SCT), suggesting that bone marrow or peripheral neutrophils are important sources of circulating LCN2/gelatinase B complex.

Serum LCN2 levels in C/EBPε knockout mice

As described above, serum LCN2 levels became 24 ± 6 % of baseline levels during neutropenic conditions in patients who underwent SCT. To investigate impact of presence of neutrophils upon circulating LCN2 concentrations in normal conditions, we examined genetically mutant mice which lack mature neutrophils. C/EBPε is a transcriptional factor which is crucial for neutrophil and eosinophil differentiation [18, 20, 22]. Given that LCN2 mRNA was abundantly expressed in human myeloid cell lines expressing C/EBPε [2, 22], we first assessed the effects of C/EBPε on promoter activity of human LCN2 gene. In

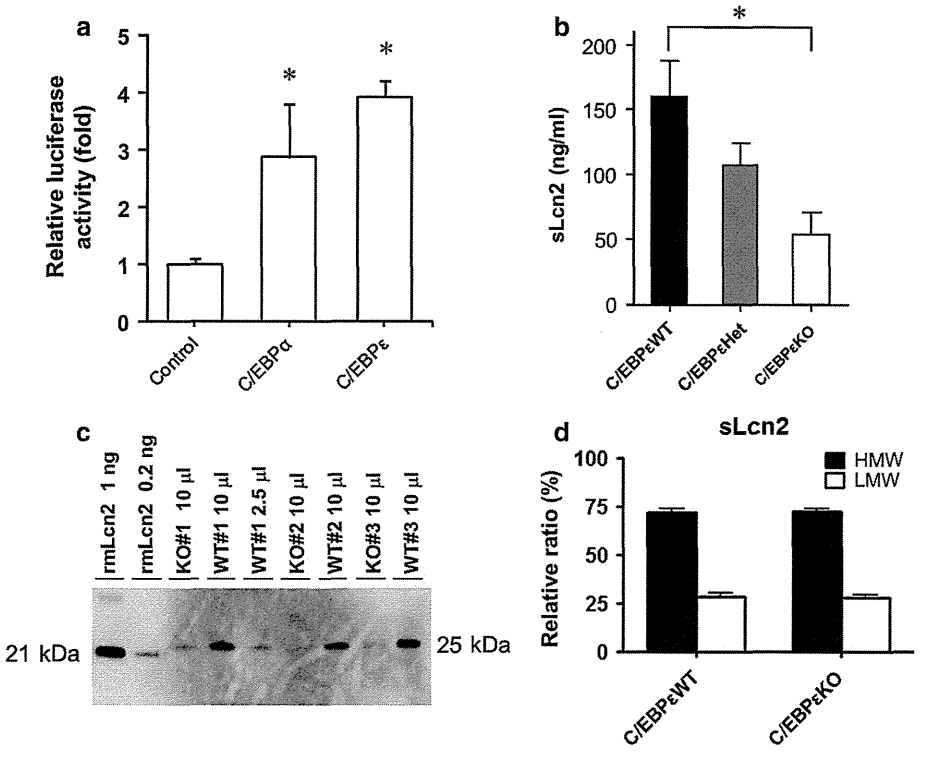

Fig. 5 C/EBPε-dependent LCN2 expression. **a** Effects of C/EBPα and ε overexpression upon human LCN2 promoter activity. Values are mean ± SEM. $n = 4$. $^*p < 0.05$ vs. control. **b** Serum total LCN2 levels including both HMW and LMW forms were measured by ELISA in C/EBPε knockout (KO), heterozygous (Het) and WT (wild-type) mice. $n = 4$. **c** Western blot analysis of serum LMW LCN2 from C/EBPε KO and WT mice (#1–3, respectively, $n = 3$). Serum aliquots (2.5 or 10 μl) from YM-100 flow through were separated by SDS-PAGE in reducing conditions. rmLCN2, recombinant mouse LCN2 as standards. **d** Relative ratios of high and low molecular weight LCN2 in the serum of C/EBPε KO and WT mice. $n = 4$

luciferase assay, overexpression of C/EBPε, as well as C/EBPα, significantly enhanced the promoter activity of LCN2 gene (Fig. 5a). Since C/EBPε$^{-/-}$ mice have severely impaired terminal differentiation of neutrophils [18, 22], these mice were utilized to determine the impact of C/EBPε-dependent neutrophil maturation on steady-state serum LCN2 levels. By ELISA, serum LCN2 levels in C/EBPε$^{-/-}$ and C/EBPε$^{+/-}$ mice were reduced by 66 ± 11 % ($p < 0.05$) and by 34 ± 12 %, respectively, as compared to C/EBPε$^{+/+}$ animals (Fig. 5b). Similar differences among genotypes were observed by Western blot of LMW (<100 kDa) fraction of the serum (Fig. 5c). These findings indicate that C/EBPε is essential for maintaining steady-state serum LCN2 levels in mice. As to molecular forms, approximately 72 % of serum LCN2 was in HMW form, and the ratio was not altered by absence of neutrophils in KO mice (Fig. 5d).

Discussion

Here, we have shown that serum LCN2 levels are decreased by 76 % during neutropenic conditions after SCT, consistently with our present findings in C/EBPε KO mice, which lack functionally mature neutrophils [18, 22]. Furthermore, serum LCN2 levels showed a strong correlation with blood neutrophil counts. These findings show, for the first time to our knowledge, that circulating neutrophils are the predominant source of steady-state blood LCN2.

LCN2 plays an essential role in host defense by inhibiting the growth of bacteria such as Escherichia coli and Mycobacterium tuberculosis [9, 23]. Therefore, not only neutropenia but also reduced circulating LCN2 levels may contribute to the high susceptibility of patients to infection during the neutrophil nadir periods after SCT. To date, it is not known whether subjects with supranormal circulating LCN2 levels are super-protected against infection.

When serum and urine LCN2 were separated into HMW and LMW forms, HMW LCN2 was the major form in blood, while urinary LCN2 consisted almost exclusively of LMW forms. These findings were quite surprising, since blood and urinary LCN2 levels are both elevated early in the course of AKI and both of these markers have been considered to be useful biomarkers of AKI [2, 6]. During nadir periods of the neutrophil counts, bacterial infection caused minimal elevation in serum LCN2 levels, but AKI lead to remarkable elevation in serum and urinary LCN2 levels. These findings suggest that the major source of serum LCN2 is the neutrophils in healthy and infected conditions, whereas the kidneys, especially the nephron segments of the thick ascending limbs of Henle and collecting ducts [2, 8, 11], are the main source of serum and urinary LCN2 in AKI. Cai et al. [24] examined molecular forms of LCN2 in the urine and reported that renal tubules mainly secrete monomer LCN2, whereas neutrophils

predominantly release dimer LCN2. Information concerning LCN2 in the blood was not provided in their work [24]. Of note, mature neutrophils contain large amount of LCN2 protein in the secretory granules but LCN2 mRNA expression is lost in these cells [1, 2, 25], making it very difficult to quantitatively evaluate neutrophil-derived LCN2 at the mRNA level. In patients with overt proteinuria (which suggests the presence of severe glomerular injury), HMW urinary LCN2 proteins were observed (Fig. 4b). At least some of HMW urinary LCN2 proteins are presumed to derive from the blood. Recently, we have been able to purify and identify several LCN2-binding proteins in the urine from patients with chronic kidney disease [26].

How is LCN2 synthesized in the kidney secreted in the blood or excreted in the urine deserves to be discussed. When we stained LCN2 protein in injured mouse kidneys in a previous study, we found 2 staining patterns [11]. One was a granular pattern along apical side of proximal tubules, which appears to reflect blood-driven, reabsorbed LCN2 protein. The other was diffusely distributed in the cytoplasm of distal nephron cells, and we speculate that LCN2 protein in this compartment is released into the urine or circulation, at least partially, through a non-specific pathway, not depending upon secretory granules. Indeed, wild-type kidney transplanted into LCN2 KO mice does release LCN2 protein in the urine (potentially through circulation) after induction of ischemic kidney injury [8].

A portion (15 %) of LCN2 in neutrophil secretory granules co-localizes with gelatinase B [3] and forms heterodimer with gelatinase B [1], preserving gelatinase B from degradation [27]. When we examined the concentration of LCN2/gelatinase B complex in the total LCN2 immunoreactivities in the blood of healthy subjects and patients undergoing SCT, the complex occupied <30 %. We also found that the ratio of the complex is largely reduced during neutropenic periods. These findings suggest that neutrophils are an important source of LCN2/gelatinase B complex in the blood but the complex only constitutes a small fraction of circulating LCN2.

There are several limitations in this study. The present study was mainly focused to longitudinal analysis of patients undergoing SCT, and the numbers of patients with hematologic or renal disorders and healthy subjects were small. Since severity of bacterial infection is generally larger when it is associated with AKI, higher peak serum and urinary LCN2 levels in Group 4 [bacterial infection (+), AKI (+)] compared to Group 2 [bacterial infection (+), AKI (−)] may have been caused not only by complicating AKI but also by more severe infection.

In conclusion, neutrophils are the predominant source of circulating LCN2 in physiological conditions, which may play an important role in the prevention of bacterial infection. In AKI, serum LCN2 proteins are dramatically increased even among patients in neutropenic states, suggesting that injured kidneys are major source of circulating LCN2 in pathologic conditions. The present study brings new insights into our understanding of the complicated regulation and clinical implication of blood or urinary LCN2 concentrations as biomarkers of AKI.

Acknowledgments The authors are grateful to Drs. K. Xanthopolous (Aurora Biosciences, San Diego, CA) and J. Lekstrom-Himes (the National Institutes of Health, Bethesda, MD) for providing C/EBPε knockout mice. C/EBP α cDNA was a kind gift from Dr. D.G. Tenen (Beth Israel Deaconess Medical Center and Harvard Medical School, Boston, MA). We also want to thank Ms. M. Nakaya (Abbott Japan, Matsudo, Japan) for discussion. This work was supported by grants from the Ministry of Education, Science, Sports and Culture of Japan (K.M., H.K. and M.M.), the Japan Kidney Foundation (K.M.), the Project Research from the High-Technology Center of Kanazawa Medical University (H.K.), the Smoking Research Foundation (M.M.), and the National Institutes of Health and A*STAR of Singapore (H.P.K.).

Conflict of interest K.M. and J.B. are a part of patent co-inventors for LCN2 as a diagnostic marker of renal failure. The other authors have no conflicts of interest to declare.

References

1. Kjeldsen L, Johnsen AH, Sengelov H, Borregaard N. Isolation and primary structure of NGAL, a novel protein associated with human neutrophil gelatinase. J Biol Chem. 1993;268:10425–32.
2. Mori K, Nakao K. Neutrophil gelatinase-associated lipocalin as the real-time indicator of active kidney damage. Kidney Int. 2007;71:967–70.
3. Cowland JB, Borregaard N. The individual regulation of granule protein mRNA levels during neutrophil maturation explains the heterogeneity of neutrophil granules. J Leukoc Biol. 1999;66:989–95.
4. Cowland JB, Borregaard N. Molecular characterization and pattern of tissue expression of the gene for neutrophil gelatinase-associated lipocalin from humans. Genomics. 1997;45:17–23.
5. Mori K, Lee HT, Rapoport D, Drexler IR, Foster K, Yang J, Schmidt-Ott KM, Chen X, Li JY, Weiss S, Mishra J, Cheema FH, Markowitz G, Suganami T, Sawai K, Mukoyama M, Kunis C, D'Agati V, Devarajan P, Barasch J. Endocytic delivery of lipocalin-siderophore-iron complex rescues the kidney from ischemia-reperfusion injury. J Clin Invest. 2005;115:610–21.
6. Mishra J, Dent C, Tarabishi R, Mitsnefes MM, Ma Q, Kelly C, Ruff SM, Zahedi K, Shao M, Bean J, Mori K, Barasch J, Devarajan P. Neutrophil gelatinase-associated lipocalin (NGAL) as a biomarker for acute renal injury after cardiac surgery. Lancet. 2005;365:1231–8.
7. Nickolas TL, O'Rourke MJ, Yang J, Sise ME, Canetta PA, Barasch N, Buchen C, Khan F, Mori K, Giglio J, Devarajan P, Barasch J. Sensitivity and specificity of a single emergency department measurement of urinary neutrophil gelatinase-associated lipocalin for diagnosing acute kidney injury. Ann Intern Med. 2008;148:810–9.
8. Paragas N, Qiu A, Zhang Q, Samstein B, Deng SX, Schmidt-Ott KM, Viltard M, Yu W, Forster CS, Gong G, Liu Y, Kulkarni R,

Mori K, Kalandadze A, Ratner AJ, Devarajan P, Landry DW, D'Agati V, Lin CS, Barasch J. The NGAL reporter mouse detects the response of the kidney to injury in real time. Nat Med. 2011;17:216–22.
9. Flo TH, Smith KD, Sato S, Rodriguez DJ, Holmes MA, Strong RK, Akira S, Aderem A. Lipocalin 2 mediates an innate immune response to bacterial infection by sequestrating iron. Nature. 2004;432:917–21.
10. Yang J, Goetz D, Li JY, Wang W, Mori K, Setlik D, Du T, Erdjument-Bromage H, Tempst P, Strong R, Barasch J. An iron delivery pathway mediated by a lipocalin. Mol Cell. 2002;10: 1045–56.
11. Kuwabara T, Mori K, Mukoyama M, Kasahara M, Yokoi H, Saito Y, Yoshioka T, Ogawa Y, Imamaki H, Kusakabe T, Ebihara K, Omata M, Satoh N, Sugawara A, Barasch J, Nakao K. Urinary neutrophil gelatinase-associated lipocalin levels reflect damage to glomeruli, proximal tubules, and distal nephrons. Kidney Int. 2009;75:285–94.
12. Bolignano D, Lacquaniti A, Coppolino G, Donato V, Campo S, Fazio MR, Nicocia G, Buemi M. Neutrophil gelatinase-associated lipocalin (NGAL) and progression of chronic kidney disease. Clin J Am Soc Nephrol. 2009;4:337–44.
13. Xu SY, Pauksen K, Venge P. Serum measurements of human neutrophil lipocalin (HNL) discriminate between acute bacterial and viral infections. Scand J Clin Lab Invest. 1995;55:125–31.
14. Martensson J, Bell M, Oldner A, Xu S, Venge P, Martling CR. Neutrophil gelatinase-associated lipocalin in adult septic patients with and without acute kidney injury. Intensive Care Med. 2010;36:1333–40.
15. Kjeldsen L, Johnsen AH, Sengelov H, Borregaard N. Isolation and primary structure of NGAL, a novel protein associated with human neutrophil gelatinase. J Biol Chem. 1993;268:10425–32.
16. Rudd PM, Mattu TS, Masure S, Bratt T, Van den Steen PE, Wormald MR, Küster B, Harvey DJ, Borregaard N, Van Damme J, Dwek RA, Opdenakker G. Glycosylation of natural human neutrophil gelatinase B and neutrophil gelatinase B-associated lipocalin. Biochemistry. 1999;38:13937–50.
17. Kanda J, Mizumoto C, Kawabata H, Tsuchida H, Tomosugi N, Matsuo K, Uchiyama T. Serum hepcidin level and erythropoietic activity after hematopoietic stem cell transplantation. Haematologica. 2008;93:1550–4.
18. Yamanaka R, Barlow C, Lekstrom-Himes J, Castilla LH, Liu PP, Eckhaus M, Decker T, Wynshaw-Boris A, Xanthopoulos KG. Impaired granulopoiesis, myelodysplasia, and early lethality in CCAAT/enhancer binding protein epsilon-deficient mice. Proc Natl Acad Sci USA. 1997;94:13187–92.
19. Radomska HS, Huettner CS, Zhang P, Cheng T, Scadden DT, Tenen DG. CCAAT/enhancer binding protein alpha is a regulatory switch sufficient for induction of granulocytic development from bipotential myeloid progenitors. Mol Cell Biol. 1998; 18:4301–14.
20. Chumakov AM, Grillier I, Chumakova E, Chih D, Slater J, Koeffler HP. Cloning of the novel human myeloid-cell-specific C/EBP-epsilon transcription factor. Mol Cell Biol. 1997;17: 1375–86.
21. Axelsson L, Bergenfeldt M, Ohlsson K. Studies of the release and turnover of a human neutrophil lipocalin. Scand J Clin Lab Invest. 1995;55:577–88.
22. Gombart AF, Kwok SH, Anderson KL, Yamaguchi Y, Torbett BE, Koeffler HP. Regulation of neutrophil and eosinophil secondary granule gene expression by transcription factors C/EBP epsilon and PU.1. Blood. 2003;101:3265–73.
23. Saiga H, Nishimura J, Kuwata H, Okuyama M, Matsumoto S, Sato S, Matsumoto M, Akira S, Yoshikai Y, Honda K, Yamamoto M, Takeda K. Lipocalin 2-dependent inhibition of mycobacterial growth in alveolar epithelium. J Immunol. 2008;181:8521–7.
24. Cai L, Rubin J, Han W, Venge P, Xu S. The origin of multiple molecular forms in urine of HNL/NGAL. Clin J Am Soc Nephrol. 2010;5:2229–35.
25. Cowland JB, Borregaard N. The individual regulation of granule protein mRNA levels during neutrophil maturation explains the heterogeneity of neutrophil granules. J Leukoc Biol. 1999;66: 989–95.
26. Nickolas TL, Forster CS, Sise ME, Barasch N, Valle DS, Viltard M, Buchen C, Kupferman S, Carnevali ML, Bennett M, Mattei S, Bovino A, Argentiero L, Magnano A, Devarajan P, Mori K, Erdjument-Bromage H, Tempst P, Allegri L, Barasch J. NGAL (LCN2) monomer is associated with tubulointerstitial damage in chronic kidney disease. Kidney Int. 2012;82:718–22
27. Yan L, Borregaard N, Kjeldsen L, Moses MA. The high molecular weight urinary matrix metalloproteinase (MMP) activity is a complex of gelatinase B/MMP-9 and neutrophil gelatinase-associated lipocalin (NGAL). Modulation of MMP-9 activity by NGAL. J Biol Chem. 2001;276:37258–65.

Human Molecular Genetics, 2015, 1–12

doi: 10.1093/hmg/ddv156
Advance Access Publication Date: 1 May 2015
Original Article

ORIGINAL ARTICLE

Seipin is necessary for normal brain development and spermatogenesis in addition to adipogenesis

Chihiro Ebihara[1], Ken Ebihara[1,5,*], Megumi Aizawa-Abe[1,5], Tomoji Mashimo[2], Tsutomu Tomita[1], Mingming Zhao[1], Valentino Gumbilai[1], Toru Kusakabe[1,3], Yuji Yamamoto[1], Daisuke Aotani[1,3], Sachiko Yamamoto-Kataoka[1], Takeru Sakai[1], Kiminori Hosoda[1,5,4], Tadao Serikawa[2] and Kazuwa Nakao[1,3]

[1]Department of Medicine and Clinical Science, [2]Institute of Laboratory Animals, [3]Medical Innovation Center, [4]Department of Health and Science, Kyoto University Graduate School of Medicine, Kyoto 6068507, Japan and [5]Institute for Advancement of Clinical and Translational Science, Kyoto University Hospital, Kyoto, Japan

*To whom correspondence should be addressed at: Division of Endocrinology and Metabolism, Jichi Medical University, Tochigi 3290433, Japan. Tel: +81 285587355; Fax: +81 285448143; Email: kebihara@jichi.ac.jp

Abstract

Seipin, encoded by *BSCL2* gene, is a protein whose physiological functions remain unclear. Mutations of *BSCL2* cause the most-severe form of congenital generalized lipodystrophy (CGL). *BSCL2* mRNA is highly expressed in the brain and testis in addition to the adipose tissue in human, suggesting physiological roles of seipin in non-adipose tissues. Since we found *BSCL2* mRNA expression pattern among organs in rat is similar to human while it is not highly expressed in mouse brain, we generated a *Bscl2*/seipin knockout (SKO) rat using the method with ENU (*N*-ethyl-*N*-nitrosourea) mutagenesis. SKO rats showed total lack of white adipose tissues including mechanical fat such as bone marrow and retro-orbital fats, while physiologically functional brown adipose tissue was preserved. Besides the lipodystrophic phenotypes, SKO rats showed impairment of spatial working memory with brain weight reduction and infertility with azoospermia. We confirmed reduction of brain volume and number of sperm in human patients with *BSCL2* mutation. This is the first report demonstrating that seipin is necessary for normal brain development and spermatogenesis in addition to white adipose tissue development.

Introduction

Seipin is a protein encoded by *BSCL2* gene whose mutation causes the most severe variety of congenital generalized lipodystrophy (CGL), also known as Berardinelli-Seip congenital lipodystrophy (BSCL) (1). BSCL is a disease characterized by a near total lack of adipose tissue from birth (2). Patients with BSCL frequently develop severe insulin resistance, hypertriglyceridemia and fatty liver (3). BSCL due to *AGPAT2* (BSCL1), *BSCL2* (BSCL2), *CAV1* (BSCL3) and *PTRF* (BSCL4) mutations have been reported so far (1,4–6). BSCL1 and BSCL 2 are the most common varieties and have been reported in patients of various ethnicities (3). However, most of the patients of African origin have *AGPAT2* mutation and those from Lebanon have *BSCL2* mutation. *BSCL2* mutation is also the major cause of BSCL in Japan (7).

1-acylglycerol-3-phosphate O-acyltransferase (AGPAT) is a critical enzymes involved in the biosynthesis of triglyceride and phospholipids from glycerol-3-phosphate. Of known AGPAT isoforms, AGPAT2 is highly expressed in the adipose tissue and its deficiency causes lipodystrophy (8). Caveolin 1 encoded by *CAV1* is an integral component of caveolae, which are specialized microdomains seen in abundance on adipocyte membranes (9). Caveolin 1 binds fatty acids and translocates them to lipid droplets. Polymerase 1 and transcript release factor (PTRF) is involved in biogenesis of caveolae and regulates expression of

Received: February 5, 2015. Revised: March 31, 2015. Accepted: April 27, 2015

caveolins 1and 3 (6). On the other hand, molecular functions of seipin, a protein encoded by *BSCL2* remain unclear although seipin seems to play a role in lipid droplet formation and be involved in adipocyte differentiation. While *BSCL2* mutations cause the most severe cases of BSCL, yet seipin remains the most mysterious lipodystrophic protein in terms of function.

Seipin is a 398 (short-form) or 462 (long-form) amino acid protein that has no similarity with other known proteins or consensus motif. Seipin has two distinct hydrophobic amino acid stretches and is speculated to have two transmembrane domains (1). It also has been shown that seipin localizes to endoplasmic reticulum in various cell lines (10–12). *BSCL2* mRNA is highly expressed in the brain and the testis other than adipose tissue in human (1). BSCL2 patients exhibit much higher rate of mild mental retardation than do other BSCL patients (13). These evidences strongly suggest physiological roles of seipin in non-adipose tissues.

In the past few years, three independent models of *Bscl2* knockout mice have been reported (14–16). All these three knockout mice exhibited severe generalized lipodystrophy, demonstrating clearly that seipin deficiency itself leads to generalized lipodystrophy *in vivo*. However, in contrast to human BSCL2 patients, all the three knockout mice had low plasma triglyceride levels. In addition, Bscl2 knockout mice showed a decrease of energy expenditure that is generally increased in human BSCL2 patients (16,17). There are also some differences between mouse and human on physiological roles of seipin in non-adipose tissues. Although depression that is not a major symptom in human BSCL2 patients was reported in male *Bscl2* knockout mice (18), no phenotypes as to mental retardation that is frequently observed in human BSCL2 patients have been reported in *Bscl2* knockout mice. While *BSCL2* mRNA is highly expressed in the brain and testis in addition to the adipose tissue in human, *BSCL2* mRNA is not highly expressed in mouse brain (11). Furthermore, teratozoospermia was reported in *Bscl2* knockout mice (19) but was not observed in our male BSCL2 patients. Instead of that, oligospermia was observed in our BSCL2 patients. Thus, a new animal model of human BSCL2 is required for further understanding of physiological roles of seipin.

In this study, we chose rat as a species for the generation of a new animal model of human BSCL2 after confirming the similarity of *BSCL2* mRNA expression pattern between rat and human. We generated a *Bscl2*/seipin knockout (SKO) rat using with the *N*-ethyl-*N*-nitrosourea (ENU) mutagenesis method (20). SKO rat has a homozygous nonsense mutation (L20X) in BSCL2 gene, which is upstream of the first transmembrane domain. SKO rats showed impairment of spatial working memory with reduction of whole brain weight and infertility with azoospermia in addition to phenotypes of lipodystrophy including hypertriglyceridemia and increase of energy expenditure. Therefore, we also analyzed brain volume and semen in human BSCL2 patients. This is the first report demonstrating that seipin is necessary for normal brain development and spermatogenesis in addition to white adipose tissue development.

Results

BSCL2 mRNA expression profiles in mouse and rat

It was reported that *BSCL2* mRNA is highly expressed in the brain and the testis in human (1). To choose an animal species that is appropriate for generating the experimental model of human BSCL2, we examined *Bscl2* mRNA expressions in various tissues in mouse and rat and compared these expression profiles with that in human. In mouse, high expression of *Bscl2* mRNA was observed in the testis but not in the brain (Fig. 1A). On the other hand, *Bscl2* mRNA was highly expressed in both the brain and the testis in rat like in human (Fig. 1B). Thus, we decided to generate a seipin knockout animal on rat background as a human BSCL2 model.

Generation of seipin knockout rat

By using ENU mutagenesis followed by MuT-POWER screening of the KURMA samples (20), we generated a seipin knockout rat with a homozygous nonsense mutation (*Bscl2*$^{sko/sko}$) in *Bscl2*, the seipin gene. *Bscl2*^{sko} mutation was T to A transition at nucleotide 239 in the third exon of *Bscl2* gene, resulted in a substitution of leucine at codon 20 by the stop codon (L20X), which is upstream of the first transmembrane domain (Fig. 1C and D). Male and female heterozygous SKO rats were intercrossed to obtain homozygous SKO animals. There were 19 homozygous WT, 50 heterozygous SKO and 26 homozygous SKO rats. This ratio did not differ significantly from the expected 1:2:1 Mendelian ratio of genotypes (number of delivery = 10, mean number of pups per delivery = 9.5; $c^2 = 1.29$, $P = 0.69$). The sex ratios also did not differ significantly from the expected ratio (male; $n = 48$, female; $n = 45$; $c^2 = 0.58$, $P = 0.45$).

The body weight in SKO rats was significantly lower than that in their WT littermates from at least 3 weeks after birth (Fig. 1E). There was no difference of body weight between heterozygous SKO rats and their WT littermates (data not shown). Although there was no significant difference in the amount of food intake and respiratory exchange ratio, the oxygen consumption was significantly higher in SKO rats compared with their WT littermates (Supplementary Material, Fig. S1A–C). When weights of various tissues were compared between SKO and WT rats, the weight in most tissues was significantly increased in SKO rats (Fig. 1F), which might be the organomegaly caused by hyperinsulinemia. In contrast, in addition to the WAT and BAT, weights in the brain and testis, where high expression of *Bscl2* mRNA was observed, were significantly reduced in SKO rats.

SKO rat develops generalized lipodystrophy

Dissection and computer tomography of SKO rat revealed the lack of WAT throughout the body (Fig 2A and B). Body composition analysis demonstrated that fat mass in both subcutaneous and intra-abdominal areas was markedly reduced while lean mass was obviously increased in SKO rats (Supplementary Material, Fig. S2A). Enlargement of skeletal muscle was confirmed by magnetic resonance imaging (MRI) (Supplementary Material, Fig. S2B). In fact, the size of epididymal WAT that is one of intra-abdominal adipose tissues and subcutaneous oil red O staining positive area were extremely reduced in SKO rats although small lipid droplets were detected in both regions (Supplementary Material, Fig. S2C and D). Consistent with this, plasma leptin concentration was markedly decreased in SKO rats compared with WT rats (Fig. 2C). BSCL2 patients lack not only the 'metabolically active' adipose tissue such as subcutaneous and intra-abdominal ones but also the 'mechanical' adipose tissue located in the bone marrow and retro-orbital areas (7,21). No adipose tissue was detected in the bone marrow and retro-orbital areas in SKO rats (Supplementary Material, Fig. S2E and F).

In contrast to WAT, interscapular brown adipose tissue (BAT) remained certain (Supplementary Material, Fig. S3A), although its weight was decreased in SKO rats (Fig. 1F). To examine whether the BAT in SKO rats is functional, we conducted cold

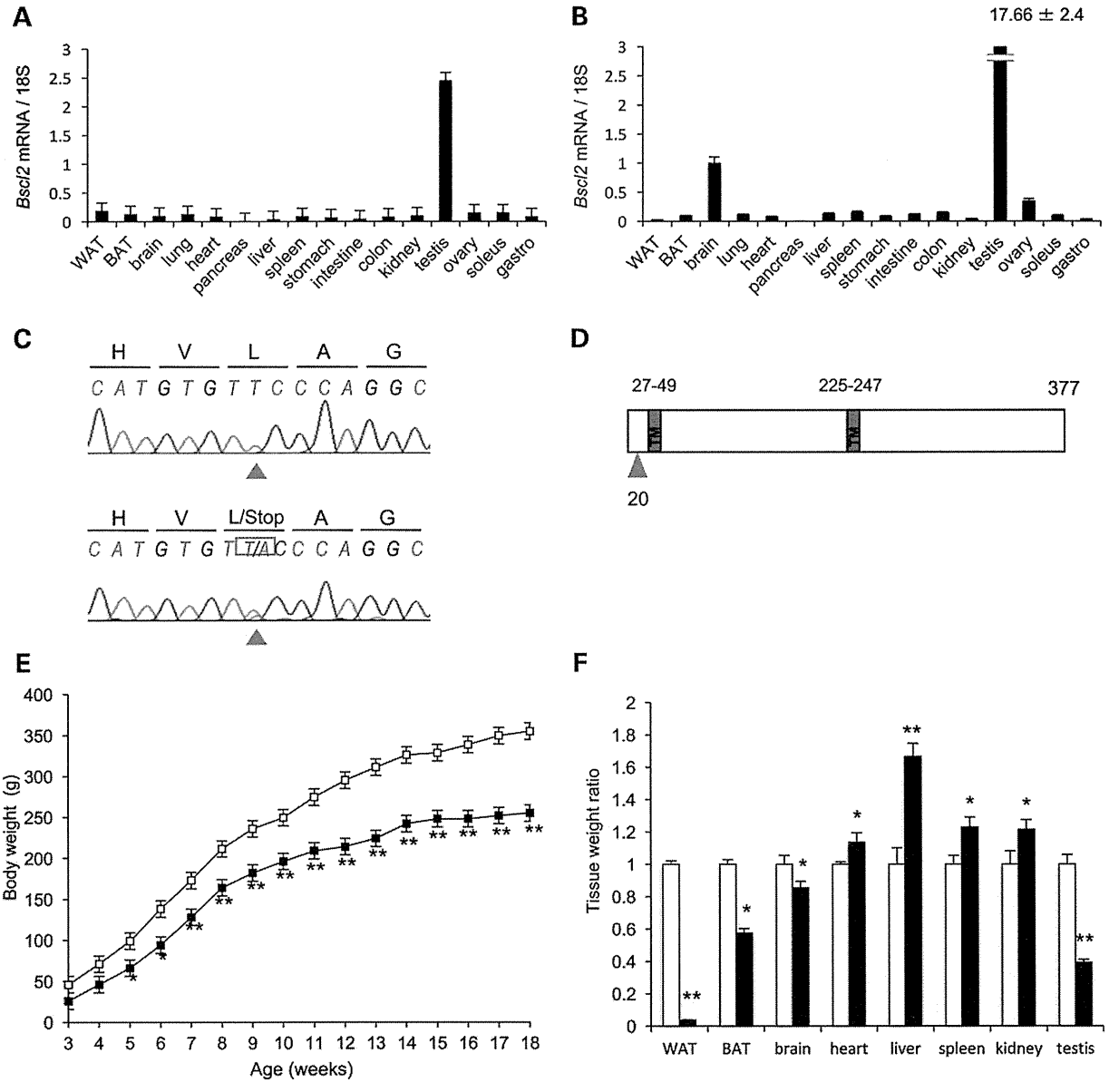

Figure 1. Development of BSCL2 animal model. (A and B) *Bscl2* mRNA expressions in various tissues in 20-week-old male mice (A) and rats (B) were checked with quantitative RT–PCR. *Bscl2* mRNA expression levels were normalized by 18S. Values are means ± SEM ($n = 10$). (C) Normal sequence and heterozygous T to A mutation at nucleotide 239 (red arrows) of *Bscl2* gene in WT and G1 male offspring heterozygous mutant rats, respectively. (D) Schematic diagram of seipin that consists of two transmembrane domains. The red arrow indicates the amino acid position of the L20X mutation. (E) Growth curve of body weight in male SKO rats (filled square) and their WT littermates (open square). Values are means ± SEM ($n = 10$ per group). $^{*}P < 0.05$, $^{**}P < 0.01$ (ANOVA). (F) Weights of various tissues in 20-week-old male SKO rats (closed bars) and their WT littermates (open bars). The fold change is displayed as relative to WT rats. Values are mean ± SEM ($n = 10$ per group). $^{*}P < 0.05$, $^{**}P < 0.01$, NS, not significant (Student's *t*-test).

exposure experiment. Twenty-four hours exposure of 4°C did not change the body temperature in both SKO and WT rats (Supplementary Material, Fig. S3B). At this time, interscapular BAT weight was similarly decreased in SKO and WT rats (Supplementary Material, Fig. S3C). Histological analysis revealed the reduction of lipid droplet number after 24 h cold exposure especially in SKO rats (Supplementary Material, Fig. S3D). In addition, increment of *Ucp1* mRNA expression by cold exposure was not just observed in both SKO and WT rats but was greater in SKO rats than in WT rats (Supplementary Material, Fig. S3E). These results indicate that the BAT in SKO rats was, in terms of thermogenesis, physiologically functional.

IPGTT showed impaired glucose tolerance with hyperinsulinemia, indicating insulin resistance, in SKO rats (Fig. 2D). Under ad lib feeding, plasma triglyceride concentration was markedly elevated in SKO rats while plasma non-esterified fatty acid (NEFA) concentration was unchanged (Fig. 2E and Supplementary Material, Fig. S4A). Plasma total cholesterol (T-Chol) was also elevated in SKO rats (Supplementary Material, Fig. S4B). We studied the effect of fasting on SKO rats. During a 24 h fasting,

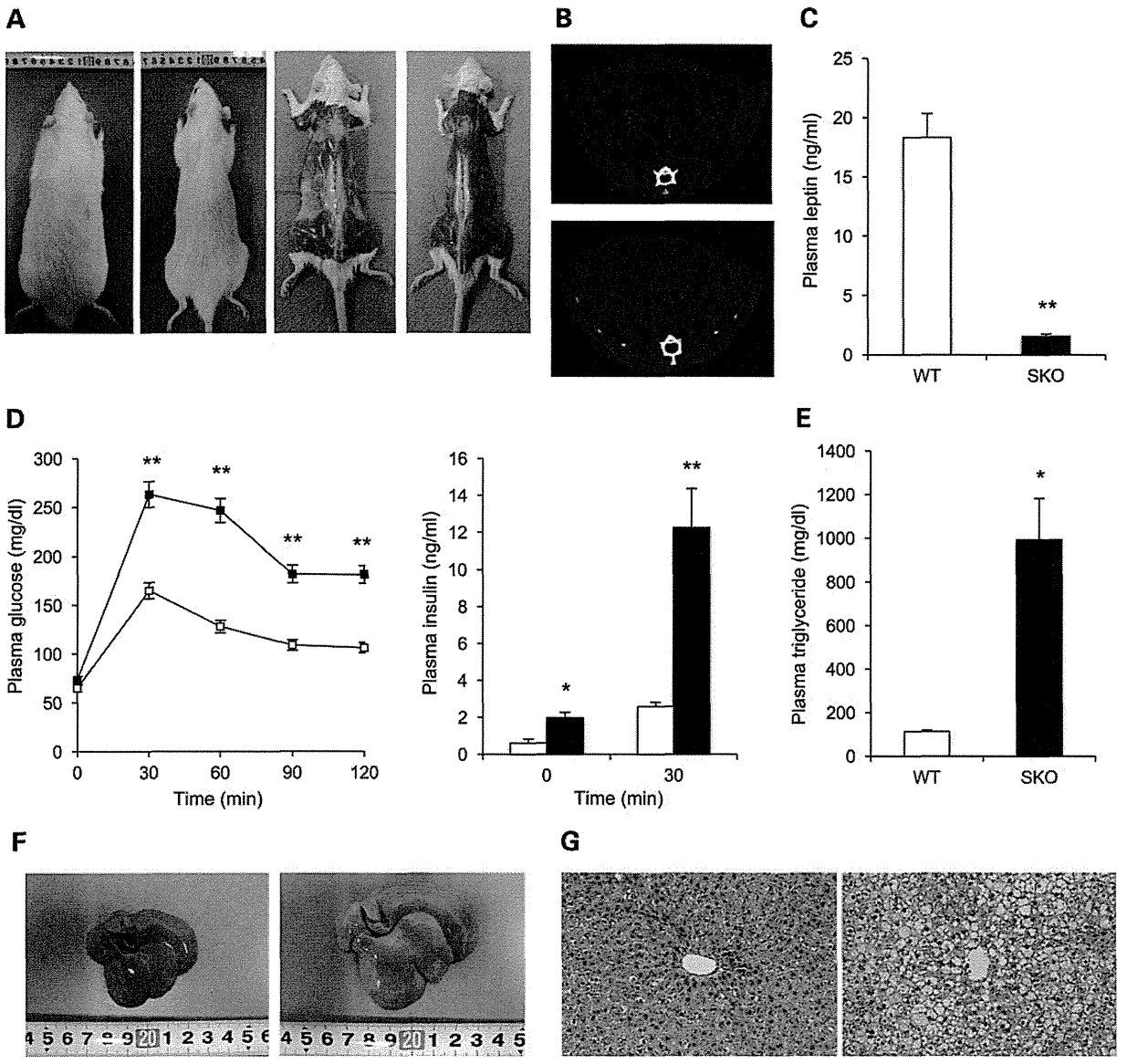

Figure 2. SKO rat develops generalized lipodystrophy. (A) Gross appearance of dorsal view before and after removal of skin in a 20-week-old male SKO rat (right) and its WT littermate (left). (B) Computer tomography image at a slice 15 cm distal from nose in a SKO rat (bottom) and its WT littermate (top). (C) Plasma leptin concentrations in SKO rats (closed bars) and their WT littermates (open bars). (D) Plasma glucose (left panel) and plasma insulin concentrations (right panel) during IPGTT in SKO rats (filled squares or closed bars) and their WT littermates (open square or open bars). (E) Plasma triglyceride concentrations in SKO rats (closed bars) and their WT littermates (open bars). (C–E) Values are means ± SEM ($n = 10$ per group). *$P < 0.05$, **$P < 0.01$, NS, not significant (Student's t-test). (F and G) Macroscopic (F) and histological images (G) of the liver in a SKO rat (right) and its WT littermate (left). For histological examination, hematoxylin and eosin staining was used. Original magnification of ×200 is shown.

both SKO and WT rats lost body weight (Supplementary Material, Fig. S5A). Glucose concentration dropped slightly in WT rats, but plummeted in SKO rats to WT levels (Supplementary Material, Fig. S5B). Insulin concentration also dropped in both SKO and WT rats although its level was still higher in SKO rats than in WT rats (Supplementary Material, Fig. S5C). Under these conditions, NEFA concentration appropriately increased in WT rats as a normal respond to fasting, meanwhile it did not increase but dropped in SKO rats, indicating that SKO rats had no sufficient lipid stores to respond to fasting (Supplementary Material, Fig. S5D). Since circulating NEFA is metabolized to ketone bodies, such as β-hydroxybutyrate, by the liver, we checked β-hydroxybutyrate concentrations. Consistent with the results of NEFA, β-hydroxybutyrate concentration vastly increased in WT rats but did not in SKO rats (Supplementary Material, Fig. S5E).

The liver in SKO rats was remarkably enlarged and was lighter in color, suggesting severe fatty liver (Fig. 2F). Histological examination showed large number of lipid droplets of various sizes in SKO rats (Fig. 2G). Consistent with these results, liver weight and liver TG content were also remarkably increased in SKO rats (Supplementary Material, Fig. S4C and D).

These results demonstrate that SKO rats develop generalized lipodystrophy and its related phenotypes, which are strikingly similar to those of human BSCL2.